

#### Contents lists available at ScienceDirect

# **Next Energy**

journal homepage: www.sciencedirect.com/journal/next-energy



#### Research article

# A novel prediction of the PV system output current based on integration of optimized hyperparameters of multi-layer neural networks and polynomial regression models



Hussein Mohammed Ridha<sup>a,b,\*</sup>, Hashim Hizam<sup>a,\*\*</sup>, Seyedali Mirjalili<sup>c,d</sup>, Mohammad Lutfi Othman<sup>a</sup>, Mohammad Effendy Ya'acob<sup>a,e</sup>, Noor Izzri Bin Abdul Wahab<sup>a</sup>, Masoud Ahmadipour<sup>f</sup>

- <sup>a</sup> Advanced Lightning, Power and Energy Research (ALPER), Department of Electrical and Electronics Engineering, Faculty of Engineering, Universiti Putra Malaysia, Serdang 43400, Malaysia
- <sup>b</sup> Department of Computer Engineering, Mustansiriyah University, Baghdad, Iraq
- <sup>c</sup> Center for Artificial Intelligence Research and Optimization, Torrens University Australia, Fortitude Valley, Brisbane, QLD 4006, Australia
- <sup>d</sup> University Research and Innovation Center, Obuda University, Budapest 1034, Hungary
- <sup>e</sup> Department of Process and Food Engineering, Faculty of Engineering, Universiti Putra Malaysia, Serdang, Selangor, 43400, Malaysia
- f School of Electrical Engineering, College of Engineering, Universiti Teknologi MARA, Shah Alam, Selangor, 40450, Malaysia

#### ARTICLE INFO

# Keywords: PV model Artificial intelligence Machine learning Deep machine learning Prediction Optimization Mountain Gazelle optimizer

#### ABSTRACT

The renewable energy system has yielded substantial enhancements to worldwide power generation. Therefore, precise prediction of long-term renewable energy conductivity is vital for grid system. This study introduces a new predictive output current for the photovoltaic (PV) system using actual experimental data. This research proposes three key contributions: The IMGO method is enhanced using several hybrid tactics to improve local search capabilities and increase exploration of significant regions within the feature space. Subsequently, the architecture of the multilayer feedforward artificial neural network is developed. The IMGO is employed to determine the appropriate hyperparameters of the model, ranging from the number of neurons in the hidden layers and learning rate. The Bayesian regularization backpropagation procedure is applied to update the weights and bias of the network. The proposed IMGO<sub>MFFNN</sub> model is ultimately combined with Polynomial regression model to improve the predictability of the PV system. The experimental results demonstrated that the proposed IMGO algorithm is very effective in addressing complex problems with high accuracy, capability, and speedy convergence. The proposed hybrid IMGO<sub>PMFFNN</sub> model proved its superior correlation evaluations, surpassing the performance of ant lion optimizer based on random forest (ALO<sub>RF</sub>) model, two stages of ANN (ALO<sub>2ANN</sub>) model, long short-term memory (LSTM), gated recurrent unit (GRU), extreme learning machine (ELM), least square support vector machine (LSSVM), and convolutional neural network (CNN) models. The MATLAB code of the IMGO is free available at: https://www.mathworks.com/matlabcentral/fileexchange/ 177214-improved-mgo-method.

#### 1. Introduction

Recent breakthroughs in renewable energy sources (RESs) have significantly advanced as a technique to mitigate pollution and climate change caused by fossil fuels use. Government and companies must transition from traditional energy sources to renewable energy sources [1]. Photovoltaic (PV) technology is regarded as one of the most

appealing sustainable energy sources for both off-grid and grid-tied applications, owning to its silent operation, renewable supply, and prolonged lifespan [2]. The efficacy of PV system is affected by several environmental conditions, such as solar radiation, ambient temperature, wind velocity, humidity, and physical attributes of the PV module. These characteristics directly influence the system's performance, often evaluated under standard test conditions (STC). Consequently, the

E-mail addresses: gs59782@student.upm.edu.my, hussain\_mhammad@uomustansiriyah.edu.iq (H.M. Ridha), hhizam@upm.edu.my (H. Hizam).

<sup>\*</sup> Corresponding author at: Advanced Lightning, Power and Energy Research (ALPER), Department of Electrical and Electronics Engineering, Faculty of Engineering, Universiti Putra Malaysia, Serdang 43400, Malaysia

<sup>\*\*</sup> Corresponding author

reliability and cost-effectiveness of PV system may be significantly enhanced by accurate and exact predicting [3].

The output prediction of the PV modules can be delineated into two phases: the first phase utilizes Machine Learning (ML) models without estimating the physical parameters of the PV module, depending on the correlation between input data (meteorological data) and output data (power or current) [4]; the subsequent phase mathematically resolves the equations of the PV model by deriving the physical parameters of the electrical equivalent circuit [5]. Obtaining genuine meteorological data across various climatic conditions, depending on location, is a means to assess and predict the output current of the PV model. A variety of models have been analyzed in the literature to clarify the correlation between climatic circumstances and physical characteristics of the PV cell, with the objective of establishing the most accurate model [6]. The predicting of PV output current may often be classified into four categories: Machine Learning, Statistical, Persistence, and Hybrid models [7]. The statistical approaches [8,9] and persistence model [7] insufficiently account for nonlinear characteristics because of computational complexity. Nevertheless, these models exhibit strong performance for a single input dataset. The ML models are susceptible to local minima and overfitting, particularly in artificial neural networks (ANNs) such as radial basis function (RBF) [10], adaptive neurofuzzy interface system (ANFIS) [11], Support vector machine (SVM) [12], long short-term memory (LSTM) [13], and extreme learning machine (ELM). These models demonstrate considerable sensitivity to the selection of the kernel functions, penalty factors, and the appropriate assignment of weights and node biases [14-16]. In contrast, when satellite data are accessible, recurrent neural networks and convolutional neural networks provide enhanced predictions [17,18]. A restricted quantity of research papers investigates the predicting of PV systems in relation to the diverse climatic variables. This is owing to the challenges that the statistical and ML models face difficulty to learn from only the historical dataset, leading to increasingly complex predictions. Furthermore, regardless to the size of the datasets used for training, adequate performance cannot be achieved [19].

Unlike stochastic optimization algorithms, ML models do not need a mathematical linking inputs to outputs. However, optimizing their hyperparameters requires more processing time [20]. Consequently, hybrid models have been widely used due to their ability to address the limitations of prior research in predicting the output current of the PV system. Liu et al. [21] introduced a genetic algorithm (GA) to improve the weights of several ANN models. The authors of [12] hybrid model consisted of wavelet transform (WT) to choose an appropriate input dataset, while particle swarm optimization (PSO) is employed to optimize the parameters of the SVM. A historical prediction series involving contiguous PV plants was conducted in [13] utilizing a GA with enhanced bidirectional LSTM model. Li et al. [19] improved the multiverse optimizer by using a chaotic sequence technique to optimally determine SVM parameters. The results indicated that the SVM model had strong performance with short-term historical data [22]. Ibrahim et al. [23] introduced ant lion optimizer (ALO) to regulate the quantity of trees and leaves in the random forest (RF) model. Density-based Spatial Clustering of Application with Noise (DBSCAN) technique is applied to remove and substitute outlier data during the training phase. Modifications are implemented for the suboptimal solutions to expedite the optimization process. Chen et al. [24] presented an online prediction model that use singular spectrum analysis (SSA) to remove noise and outliers from the input dataset. The improved PSO is then implemented to enhance the parameters of the kernel in the ELM model. The authors of [25] suggested a GA to update the weights of the nonlinear auto-regressive neural network with exogenous input (NARX). The experimental findings demonstrated a suitable level of accuracy. Nevertheless, improving the weights of NARX does not provide a significant improvement in the output accuracy. Yadav et al. [26] employed five different ANN models and various linear regression models to predict one-minute intervals of PV output power, Nevertheless, the

authors applied only a single layer with manually adjusted neuron numbers in the hidden layers, leading to unsatisfactory performance.

ALO was implemented in [27] to ascertain appropriate weights and biases for ANN model. An additional ANN was utilized to predict the output power of PV system. The results exhibited more accuracy than ANN and GA<sub>ANN</sub>, respectively. However, enhancing just the weights and biases is inadequate for predicting the output power of the PV system. Consequently, these parameters are only adjusted using a single-hidden layer [28]. Furthermore, the design of ANN significantly influences the transfer of information from input to output, thereby affecting the system's accuracy. Conversely, the prudent selection of neurons in the hidden layers may mitigate redundancy in the parameter space solutions, thereby diminishing the sensitivity of these solutions to the resulting parameters in comparison to traditional learning models [29]. Considering that a limited number of neurons may lead to poor performance, while many neurons may cause overfitting [30]. Consequently, the appropriate number of neurons in each layer should be judiciously selected to provide precise predictions for the real-world applications of the PV system [31].

The complexity of the correlation between the parameters have been extensively verified using both linear and nonlinear regression models [32]. The authors of [33] proposed ANN model to predict the PV module's output current on bright and overcast days using actual measured data collected from Marmara University, Istanbul, Turkey. The results were compared using various regression models. In [34], proposed multiple linear regression model to predict different PV modules' output in Chile region. However, the previous models may produce a notable amount of inaccuracy when the long-term of the data are obtained. Deep ML model based on ELM is proposed in [35] to characterize the electrical behavior of the PV module using different types of PV technologies. This study found that the best number of the neurons is 450 for a single hidden layer, which results accurate prediction for the large data sets of the I-V curves. A dynamic/adaptive K-Nearest Neighbor model using is proposed in Ref. [36] to estimate the efficiency of grid-connected PV system at Hashemite University. The proposed model proved its superiority over numerous methods from the literature using various statistical measures. In [37], a convolutional neural network (CNN) based on Pixel-wise Voting Network software is proposed to predict the output power of the PV module, utilizing temperature and solar radiation as inputs and the historical PV power as output, which achieved acceptable outcomes. The authors of [38] proposed ELM for PV output power prediction in a real case study conducted in Amman, Jordan. The proposed algorithm demonstrated a superiority over a back propagation neural network. Qing et al. [39] suggested a LSTM model to predict hourly daily solar radiation. According to the outcomes, the LSTM model achieved better performance than various models mentioned in the literature [40]. Yuan et al. [41] proposed a hybrid model integrating of improved butterfly optimization method, adaptive boosting, and relevance vector machine (IBOA-AdaBoost-RVM) to predict the output power of the wind turbine. The proposed model confirmed its superiority compared to other hybrid models via various statistical evaluations. The summary of the literature review is provided in Table 1.

Numerous real-world applications may be represented as optimization problems involving constraints and decision variables, using nonlinear and high-dimensional objective functions. Meta-heuristic algorithms can effectively tackle these problems because of their adaptability, simplicity, derivative-free nature, and preventing of local optima entrapment [42]. These algorithms, on the other hand, cannot provide global solutions for real-world problems, limiting their uses. To increase the applicability of current algorithms, they must be improved in terms of performance, accuracy, and trade-off between the exploration and exploitation stages [43]. The meta-heuristic algorithms have been extensively implemented to solve real-world optimization problems, including photovoltaic models [44], economic load dispatch problem [45], cloud computing [46], civil engineering [47], multi-

 Table 1

 Summary of the literature review

cummar y	y or the inerature review			
Refs.	Predictive models	Data processing	Forecast Horizon	Results
[6]	MLNN based on GNBR	Normalized	Long term	The output current of the PV model is estimated using datasheet information and optimized MLNN using Gauss-Newton approximation to Bayesian Regularization. The inputs to the model are $I_{x}$ , $V_{cc}$ , $MPP$ , $I_{mp}$ , and $V_{mp}$ , while the estimated parameters are $R_{p}$ , $I_{ph}$ , $R_{s}$ , and $I_{o}$ . These parameters are then substituted in equivalent electrical circuit of the PV model to predict the output current. The results indicated good performance of the proposed model.
[8]	Multi-task learning	Tukey approach and KNN method	Long term	This work employed a Gaussian process time-based series to predict the output power of the PV system in four schools located in Hawaii. The outliers are eliminated using Tukey approach, while K-nearest-neighbors (KNN) technique is utilized to substitute the outliers in raw dataset. Ultimately, the ARIMA model is implemented to anticipate the most generic class of time series PV data.
[10]	RBF	None	Medium term	The RBF is utilized to predict the cell temperature of the single diode (SD) PV model, using solar irradiance, ambient temperature, and wind speed as inputs. Next, using datasheet information, the output power is calculated using the projected cell temperature in an analogous electrical model. The performance results are corroborated by experimental data.
[12]	WT-PSO-SVM	WT	Short term	This research utilizes the wavelet transform (WT) for data reprocessing. The Numerical Weather Prediction (NWP) incorporates solar radiation, ambient temperature, cloud cover, humidity, atmospheric pressure and wind speed, as input data. The output PV power is derived from Supervisory Control and Data Acquisition (SCADA). The future PV output power is forecasted using WT-PSO-SVM model. The proposed model confirmed its superiority compared with other models referenced in the literature.
[13]	GA-improved BiLSTM	Normalized	Ultra-short term	This study utilizes a range of adjacent BV plants as input data, with the actual PV power serving as the output. The GA is applied to enhance the parameters batch size, layers, and units per layer of the BILSTM model. The proposed model illustrated superior accuracy compared to well-established models in the literature.
[15]	(ECBO-VMD)-PSR-(ECBO-ELM)	ECBO-VMD	Ultra short term	The proposed model in this study is accomplished by several steps: Initially, the training data for solar radiation and PV power are acquired by grey correlation analysis and Pearson correlation coefficient methods. The improved colliding bodies algorithm (ECBO) is subsequently presented to optimize the parameters of the variational mode decomposition (VMD) algorithm, where the weighted-permutation entropy is employed to formulate the cost function. Finally, the ECBO algorithm is re-implemented to enhance the ELM model. The proposed model is validated by several straistical metrics.
[16]	Self-adaptive model	Kernel density estimation method		This research uses the Kernel density estimation approach to model the forecasting error throughout the days. subsequently, the PSO method is applied to optimize the window width of the KDE. The self-adaptive dynamic model showed its superiority over the BP, SVM, and ELM models.
[17]	HQC-GRU	НОС	Long term	This study utilizes the quality of context (QoC) technique to gather meteorological data, while using the Gated Recurrent Unit Neural Network to medict the PV output power. The proposed model exhibited superior accuracy relative to the LSTM model.
[18]	QK-CNN	Linear interpolation and normalization	Ultra short term	This research employs the quadruple-kernel CNN module to extract the local features among components with differing timesteps in the sequence of input, while the single kernel CNN module is obtained to further extract local features of first step. The final forecasting is performed by combining the local and global characteristics of the target sequence.
[19]	німуо-ѕум	Normalized	Short term	An improved multi-verse optimization algorithm based on SVM is proposed to predict the output power of the PV system, employing real experimental data gathered from DKA solar center. Australia. The penalty factor and kernel function are optimized by HIMVO. The proposed method showed superior performance relative to existing models under sunny, cloudy, and rainy conditions.
[21]	Hybrid model	EVGFM	Short term	The novelty of this work is realized into two stages: First, the GRNN, ELM, and ENN are merged with GA-BP to develop weight varying combination forecast mode (WVCFM) model. Subsequently, the WVCFM model is used to provide deterministic point prediction. Secondly, the nonparametric KDE is adapted to estimate the prediction intervals. The proposed model, evaluated using four types of PV output power, demonstrated elevated levels of confidences.
[22]	FCM-WOA-LSSVM-NPKDE	FCM	Short term	This work first applies Fuzzy c-means for data clustering, followed by use of WOA to optimize penalty factor and kernel function of the LSSVM.  The NPKDE is utilized to compute the probability density distribution of forecasting error. The results indicated the superiority of the WOA-LSSVM relative to other models referenced in the literature.
[23]	DBSCAN-ALO-RF	DBSCAN	Ultra short term	DBSCAN is applied to detect the outliers, which are then removed and replaced. ALO then optimized the hyperparameters of the RF. The proposed model exhibited superiority over the other models referenced in the literature.
[24]	VMD-DAIWPSO-PSR-KELM	SSA, VMD, and PSR	Short term	This work employs singular spectrum analysis (SSA) to remove outliers, utilizes variational decomposition mode (VDM) to mitigate uncertainty and irregularity, and applies phase space reconstruction (PSR) to capture the dynamical features for the generation of suitable input-output data. The improved PSO is addressed to extract the optimal parameters of PSR and KELM. The proposed hybrid model is verified by commaniant it with some marbods using experimental data.
[25]	GA-NARX	Normalized	Ultra short term	by comparing a war seven increases again superior again. The GA is employed to optimize the weights and biases of the nonlinear auto-regressive recurrent neural network with exogenous inputs (NARX) using real experimental data collected from Algerian electricity and DKASC in Australia. The results shown that the proposed model offers very good estimate using relative RMSE.
[27]	VDM-ACO – 2ANN	VDM	Short term	This research use the VDM for data processing. Then, the ACO is implemented to optimize the weights and biases of the ANN. The proposed model is evaluated using a PV power system in Beijing, China and outperformed other models documented in the literature.
[34]	MLR	Pearson coefficient	Ultra long term	This work reprocesses the data using Pearson coefficient to identify the representative variables for the energy production of the PV system. The Performance Ratio (PR) is then computed. The multiple linear regression (MLR) is applied to predict the output PV power.

e output PV power.
(continued on next page)

$\leq$	۰
7	١
continued	
=	۹
- 5	
.5	1
+	ì
2	٠
~	ī
	1
. •	ė
_	•
_	
٩	
_	۰
_	1
ď	
Ë	

Refs.	Refs. Predictive models	Data processing	Forecast Horizon	Results
[32]	ЕГМ	Resampling and normalization methods	Long term	This research enhances data quality and eliminates noisy data points using linear resampling of the I-V data curves. The irradiation-temperature grid method is implemented to downsample the datasets. Then, the ELM is applied to predict the I-V curves for various types of PV modules. The proposed method is tested using many statistical metrics and compared against BDNI, GRNN, SRM, RF, and DE.
[36]	Adaptive K-NN	Manual cleaning	Medium term	This paper uses a dynamic/adaptive K-nearest Neighbor (K-NN) model to assess conversion efficiency of the PV system. The condition's weights are identified by their resemblance to the test pattern. The proposed model surpassed ANN, ELM, and MLR in performance.
[37]	CNN-PVPNet model	Normalized	Short term	In this study, the Conventional neural network using PVPNet model is presented to predict the output power of the PV system. The proposed model is compared with SVM, RF, decision tree, MLP, and LSTM.
[38]	ELM	Manual processing- normalized	Short term	ELM is presented to predict the power output of the PV system using real experimental data collected from the Faculty of Engineering at the Applied Science University, Amman, Jordan. The proposed model surpassed BP-ANN model in performance.
[36]	LSTM	Normalized	Short term	The LSTM is employed to predict hourly day-ahead solar radiation. The experimental findings indicated the superiority of the LSTM over persistence, linear least squares regression (LR), and BPNN models.
[40]	Adam-UPSO-LSTM	Pearson model	Short term	This study proposes the Adam optimizer based on a unified PSO algorithm to optimize the weights of the LSTM model. The experimental findings demonstrated the superiority of the proposed model relative to those documented in the literature.
[41]	IBOA-AdaBoost-RVM	Normalization and Pearson model	Short term	This research normalizes the data and the Pearson model is applied to assess the correlation between the variables. The AdaBoost is used to augment the weights of individual samples, RVM is employed to eliminate the overfitting during training, and IBOA is applied to enhance the hyperparameters of the model.

Hybrid improved multi-verse optimization algorithm; Kernel-based Extreme particle swarm optimization; PV = photovoltaic; RBF = radial basis function; RF = random forest; SVM ALO = ant lion optimizer; ANN = artificial neural network; CNN = convolutional neural network; DBSCAN = Density-based Spatial Clustering of Application with Noise; ELM = extreme learning machine; GRU = Whale Optimization Algorithm; NPKDE = Non-parametric kernel Density Estimation; DAIWPSO = Dynamical Adjustment of the Inertia Weight PSO; KELM = Regularization; HQC = high quality context; HIMVO = gated recurrent unit; LSSVM = least square support vector machine; LSTM = long short-term memory; PSO = support vector machine; MLNN = Multilayer Neural Network; GNBR = Gauss-Newton Based on Bayesian Learning Machine; UPSO = Unified Particle Swarm Optimization; IBOA = Fuzzy c-means; WOA

microgrid systems [48], and others [49]. According to the No Free Launch theory [50], there is no specific algorithm can handle all optimization problems. Therefore, there is still a roam for further developments in order to improve the exploration/exploitation tendencies [51]. The majority of research papers utilize hybridization of several ML approaches to predict the PV power output without considering the values of the hyperparameters, which might have a direct impact on the proposed model's accuracy [52]. Moreover, most of authors improved the weights and bias of the ANN model, which did not provide a greater accuracy as compared to development in the ANN's structure. Finally, employing only multiple regression models can result a modest degree of accuracy [53]. According to the previous, we have developed the original Mountain Gazelle Optimizer (MGO) using several powerful strategies in order to achieve a balance between the exploration and exploitation tendencies. Then, the Improved Mountain Gazelle Optimizer (IMGO) is applied to enhance the hyperparameters of the multiple feed-forward neural network, including number of the neurons in the three hidden layers and learning rate. In addition to that, the proposed IMGO<sub>PMFFNN</sub> model is integrated with polynomial regression model based on linear square method to precisely predict the output current of the PV module under various environmental conditions. The proposed IMGO<sub>PMFFNN</sub> is verified by various well-published models. a new model to precisely predict the PV model output current using real experimental data. The contributions of this study can be highlighted as

In terms of developments of MGO algorithm:

- The improvements of the MGO is undertaken with the objective of enhancing both the exploration and exploitation stages.
- The multi-migration searching strategy (MMSS) is newly developed based generalized opposition based learning (GOL) and gaussian mutation mechanisms, which can considerably reduce slipping into local minima and increase the variety of solutions in the exploration phase.
- The multi-strategy bachelor male herds (MSBMH) is proposed using Levy flight and GOL strategies to boost the convergence to global solution while considering the information of best optimal solutions for enhancing exploitation phase.
- By upgrading the upper and lower limits based on a transformation
  of the solutions from locally to globally using the best optimum
  information, the exploitation phase in sufficiently enhanced. With
  this strategy, the quality of and diversity of solutions are developed
  for all iterations during the optimization process.
- Finally, the convergence rate is boosted by shifting the four newly generated solutions from external to internal loops.

In terms of predicting of PV output power:

- The architecture of the multiple feed-forward neural network (MFFNN) is improved to precisely handling the data during training.
- The IMGO method is employed to optimize the number of neuros in the hidden layers and learning rate, while the Bayesian regularization backpropagation algorithm is applied for updating weights and biases.
- The Polynomial Regression based on linear least square method is applied to predict final output current of the PV system.

The IMGO is verified by standard unimodal, multimodal, and fixed-dimensional benchmark functions, compared against several methods, and applied to solve six engineering design problems. Moreover, the proposed  $\rm IMGO_{\rm PMFFNN}$  model is validated using various hybrid models using real experimental data.

The present paper is structured in the following manner: The equivalent circuit of the PV model is presented in Section 2. The methodology of the basic principle, mathematical equations, improvements of the MGO, hybrid model for predicting output current of the PV

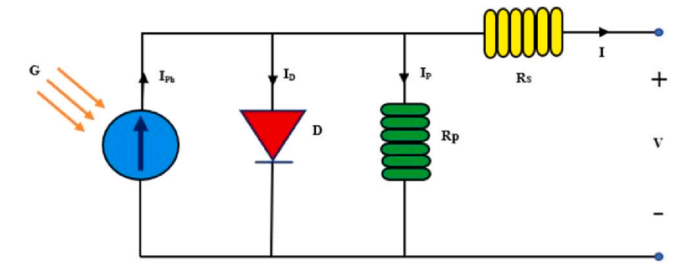


Fig. 1. The equivalent circuit of 1D-PV model. PV = photovoltaic.

system, and assessment criteria are expounded upon in Section 3. The evaluation and application of IMGO method, and performance of the proposed hybrid model for predicting output PV system are presented in Section 4. Section 5 summaries the achievements of this work and the future work direction.

#### 2. Equivalent circuit of PV model

The solar radiation and ambient temperature have a direct effect on the operation of the PV cell, where each cell conducts DC current during the day and the diode in opposite direction is activated at night. The electrical circuit of the single diode (1D PV) model is depicted in Fig. 1. The 5 physical parameters of the 1D PV model may be mathematically described as follows [54]:

$$I = I_{Ph} - I_o \left[ \exp\left(\frac{V + IR_s}{V_t}\right) - 1 \right] - \frac{V + IR_s}{R_p}$$
(1)

where  $R_s$  and  $R_p$  are series and parallel resistances. The thermal voltage  $(V_t)$  can be computed as follows:

$$V_t = \frac{dKBT_c}{q} \tag{2}$$

where KB and q are Boltzmann's constant  $(1.38 \times 10^{-23} J/K)$  and electron charge  $(1.60 \times 10^{-19} C)$ , respectively. The  $T_c$  is the cell temperature (K). The short-circuit current  $(I_{sc})$  and open-circuit voltage  $(V_{oc})$  are computed as follows [23]:

$$I_{sc} = I_{Ph} - I_o \left[ \exp\left(\frac{V + I_{sc}R_s}{V_t}\right) - 1 \right] \times \frac{R_p}{R_s + R_p}$$
(3)

$$V_{oc} = R_p \times \left( I_{Ph} - I_o \left[ \exp\left(\frac{V_{oc}}{V_t}\right) - 1 \right] \right)$$
(4)

Therefore, the current at maximum power point ( $I_{mpp}$ ) may be expressed as follows [23]:

$$I_{mpp} = I_{Ph} - I_o \left[ \exp\left(\frac{V_{mpp} + I_{mpp}R_s}{V_t}\right) - 1 \right] - \frac{V_{mpp} + I_{mpp}R_s}{R_p}$$
 (5)

Consequently, the  $P_{mpp}$  is computed by multiplying  $I_{mpp} \times V_{mpp}$ .

#### 3. Methodology

#### 3.1. Mountain Gazelle optimizer (MGO)

The MGO is found throughout a considerable portion of the Arabian Peninsula and its surroundings, but its prevalence is small. There are three main groupings of gazelles are the mother-offspring hers, young male herds, and single males' territory. In the wild, gazelles regularly move in search of food throughout a 120 km broad territory, running at speeds of up to 80 km [55]. The following expression are modeled to mathematically describe the lives of MGO: bachelor male herds, maternity herds, solitary males, and movement in search of food.

#### • Territorial solitary males

The robust and mature gazelle establishes a solitary territory, and the adult males work to maintain their location, as expressed by the following:

$$TSM = m_g - |(ri_1 \times BH - ri_2 \times X(t)) \times F| \times C_i$$
(6)

where  $m_g$  and  $ri_{1-2}$  are the locations of the global solution and random values 1 or 2 [55]. BH, F, and  $C_i$  are coefficients of the young male herd, control parameter, and randomly number updated in each iteration, which may be acquired to improve the searching ability [55], as follows:

$$BH = X_{ra} \times r_1 + M_{pr} \times r_2, ra = \left\{ \left\lceil \frac{N}{3} \right\rceil ... N \right\}$$
(7)

where  $X_{ra}$  is randomly picked within the range of ra,  $M_{pr}$  is the average number of search agents chosen at random  $\left\lceil \frac{N}{3} \right\rceil$ , N is the total number of solutions, and  $r_{1-2}$  are randomly selected between 0 and 1.

$$F = N_1(D) \times \exp\left(2 - t \times \left(\frac{2}{T}\right)\right) \tag{8}$$

where  $N_1$  is the standard distribution selected at random. t and T are the current and maximum iterations.

$$C_{i} = \begin{cases} (a+1) + r_{3} \\ a \times N_{2}(D) \\ r_{4}(D) \\ N_{3}(D) \times N_{4}(D)^{2} \times \cos((r_{4} \times 2) \times N_{3}(D)) \end{cases}$$
(9)

where  $r_3$  and  $r_4$  are return random scalar obtained from a uniform distribution of the interval (0, 1).  $N_2$ ,  $N_3$ , and  $N_4$  are integers drawn at random from the population, while a is computed as follows [55]:

$$a = -1 + t \times \left(\frac{-1}{T}\right) \tag{10}$$

### • Maternity herds

The maternity herds are responsible for producing packs that give birth to sturdy males, in which may influence the delivery of young males to occupy females, as modeled by the following:

$$MH = (BH + C_{1r}) + (ri_3 \times m_g - ri_4 \times X_r) \times C_{2r}$$
 (11)

where BH is the impact factor's vector of young male,  $C_{1r}$  and  $C_{2r}$  are selected at random to compute the independently,  $r_{i_3}$  and  $r_{i_4}$  are random numbers 1 or 2 [55], and  $X_r$  is vector selected at random from population.

#### • Bachelor male herds

Once the male gazelles become mature, they establish territories and seize control of the females. The young gazelles use aggression to dominate female gazelles and it is given by the following [55]:

$$BMH = (X(t) - D) + (ri_5 \times m_g - ri_6 \times BH) \times C_r$$
 (12)

where X(t) represents the gazelle's location in the current iteration,  $r_{i_5}$  and  $r_{i_6}$  are random numbers 1 or 2 [55], and D is computed as follows:

$$D = (|X(t)| + |m_g|) \times (2 \times r_6 - 1)$$
(13)

where  $r_6$  is randomly selected within range of 0 and 1.

• Migration to search for food

The Mountain Gazelles, which have a fast running speed and strong leaping, are in charge of providing food supplies. This behavior is formulated as follows:

$$MSF = (ub - lb) \times r_7 - lb \tag{14}$$

where ub and lb are the upper and lower limits, and  $r_7$  is a random values between 0 and 1 [55]. Consequently, the four TSM, MH, BMH,

and *MSF* tactics are applied to generate new solutions. The population is expanded to include the additional four vectors, after which the solutions are arranged in ascending order. Then, the weakness solutions are removed from the current iteration. This process will continue until the stopping criteria is satisfied.

#### 3.2. The proposed improved MGO

#### • Mult-migration strategy searching for food

In the basic MGO, the Migration Search Food step has weakness in terms of looking for of new potential areas. This is because the newly created solutions consider only the lower and upper borders. Therefore, the new MMSS depends on fast sprinting and forceful leaping of gazelles by implementing the *GOL* strategy mechanism to sufficiently escape from neighborhood and improve the propensity for exploration at the first stage of half number population size [56], whereas the gaussian mutation is applied in the rest for increasing the diversity of solutions in the exploratory phase. Moreover, the GOL tactic utilizes upper and lower limits of the current vector iteration to prevent the loss of highly solutions quality during the exploitation stage. Therefore, the MMSS may be expressed as follows:

$$MMSS = \begin{cases} m_g - C_r \times (GOL - X_r) + C_r \times (X(t) - r \times X_r) ifi < N/2 \\ X(t) \times (1 + rn) otherwise \end{cases}$$
 (15)

where  $GOL = r \times (A_t + B_t) - X(t)$ , rn returns a random scalar obtained from a uniform distribution of the interval (0, 1), and

$$GOL \in [A_t, B_t]; j = 1, 2, ..., N$$
 (16)

where  $A_t$  and  $B_t$  are the upper and lower variables of the current iterations. Therefore, the  $[A_t, B_t]$  are dynamically updated during the optimization process in order to prevent premature convergence and local minima [57].

# • Mult-strategy bachelor male herds

The exploiter mechanism acts with a poor performance, where the optimizer MGO struggles to escape from local minima and reach globally. Therefore, the MSBMH step is officially formulated by considering the neighborhood information around the best optimal solution with including the levy flight (*Levy*) movements when the number of iterations is less than half number of population size, while the rest is addressed by the *GOL* [58]. In this way, the searching mechanism is ensured by utilizing multi-explore strategy for looking for new promising zones and avoiding premature convergence, as represented by the following:

$$MSBMH = \begin{cases} m_g - ((X_r) + Levy \times X(t))ifi < N/2 \\ m_g - (M - GOL) \times C_r otherwise \end{cases}$$
 (17)

where Levy is a step sizes chosen randomly using a probability function [59]. The Levy is computed as follows:

$$Levy(\alpha) \approx |x_j|^{1-\alpha} \tag{18}$$

where  $x_j$  refers to the flight's length, while the exponent of the power-law is between  $1 < \alpha < 2$  [60]. The Levy's probability density in the integral form is represented by [61],

$$f_L(x, \mu, \sigma) = \frac{1}{\pi} \int_0^\infty \exp(-\gamma q^\alpha) \cos(qx) dq$$
 (19)

where  $\alpha$  denotes to the distribution index which controls the cale properties of the process,  $\gamma$  is utilized for selection of the scale unit. The integral is employed when  $\alpha=2$  represents the Gaussian distribution, and when  $\alpha=1$  represents a Cauchy distribution [62]. The series expansion method is essential when x has a large value, as given below:

$$f_L(x, \mu, \sigma) = \frac{\gamma \Gamma(1 + \alpha) \sin\left(\frac{\pi \alpha}{2}\right)}{\pi x^{(1+\alpha)}}, x = \infty$$

where  $\Gamma$  is Gamma function in which  $\Gamma(1+\alpha)$  is equal to  $\alpha$ !. According to [61], the  $\alpha$  value is ranged within 0.3 and 1.99. Therefore, the Mantegna method is applied to conduct a random value utilizing Levy distribution, as described below:

$$Levy(\alpha) = 0.05 \times \frac{x}{|y|^{1/\alpha}}$$
(20)

where x and y are 2 normal distributions values and given by the following:

 $x = Normal(0, \sigma_x^2)$ , and  $y = Normal(0, \sigma_y^2)$ , where  $\sigma_x$  is calculated by the following:

$$\sigma_{x} = \left[ \frac{\Gamma(1+\alpha)n\left(\frac{\pi\alpha}{2}\right)}{\Gamma\left(\frac{(1+\alpha)}{2}\right)\alpha 2^{\left(\frac{\alpha-1}{2}\right)}} \right]^{1/\alpha}$$
(21)

where  $\alpha = 1.5$  and  $\sigma_y = 1$ . The Levy tactic has motions with small steps size combined with large jumps.

• Gazelle traveling from locality to optimal new territory

After the 4 *TSM*, *MH*, *MSBMH*, and *MMSS* tactics produce the new solutions, their boundaries are updated using straightforward mechanism by returning either maximum or lowest value of each variable, which delays not only the search for the best solution but also postposes the convergence rate. Therefore, the new strategy imposes the new gazelle to gather information from the male gazelle (best solution) while increasing the diversity by integrating the upper and lower variables to avoid falling in locality. In the other words, the newly generated solutions are strengthened in light of best solution found so far, as expressed by the following [5]:

$$X(t) = \begin{cases} m_g - \epsilon \times (\mathbf{r} \times (ub - lb)) \text{ if } X(t) > ub(t) \\ \epsilon \times (\mathbf{r} \times (ub - lb)) + m_g \text{ if } X(t) < ub(t) \\ X(t) \text{ otherwise} \end{cases}$$
(22)

where  $\varepsilon$  is a small integer number [63].

• Accelerating the convergence rate

Adding the four new generating solutions, at the end of maximum iteration, in the basic MGO to the existing population leads to delay the optimization process, and the population size becomes very large without any gains. As a consequence, the solutions are sorted and weakness solutions are removed after each new iteration, which leads to boost the convergence rate. The flowchart of the IMGO is demonstrated in Fig. 2.

The performance of the proposed IMGO algorithm on solving benchmark functions and solving engineering problems are provided in Supplementary Materials.

# 3.3. Hybrid model for predicting output power of the PV system

This section presents a description of the proposed  $IMGO_{PMFFNN}$  model by employing IMGO to optimize the hyperparameters of the MFFNN, including number of neurons in the hidden layers and learning rate. Afterward, the Polynomial regression model is hybridized to predict the output current of the PV module.

# 3.3.1. Artificial neural network (ANN)

ANN can be considered an information processing system that models human nervous activities impacted by the neuronal connection and behavior [64]. ANN can tackle difficult problems effectively due to its capacity to cope with nonlinear relationships between the input and output variables, where learning process has a substantial influence on its effectiveness [65]. The primary models of the multilayer perceptron

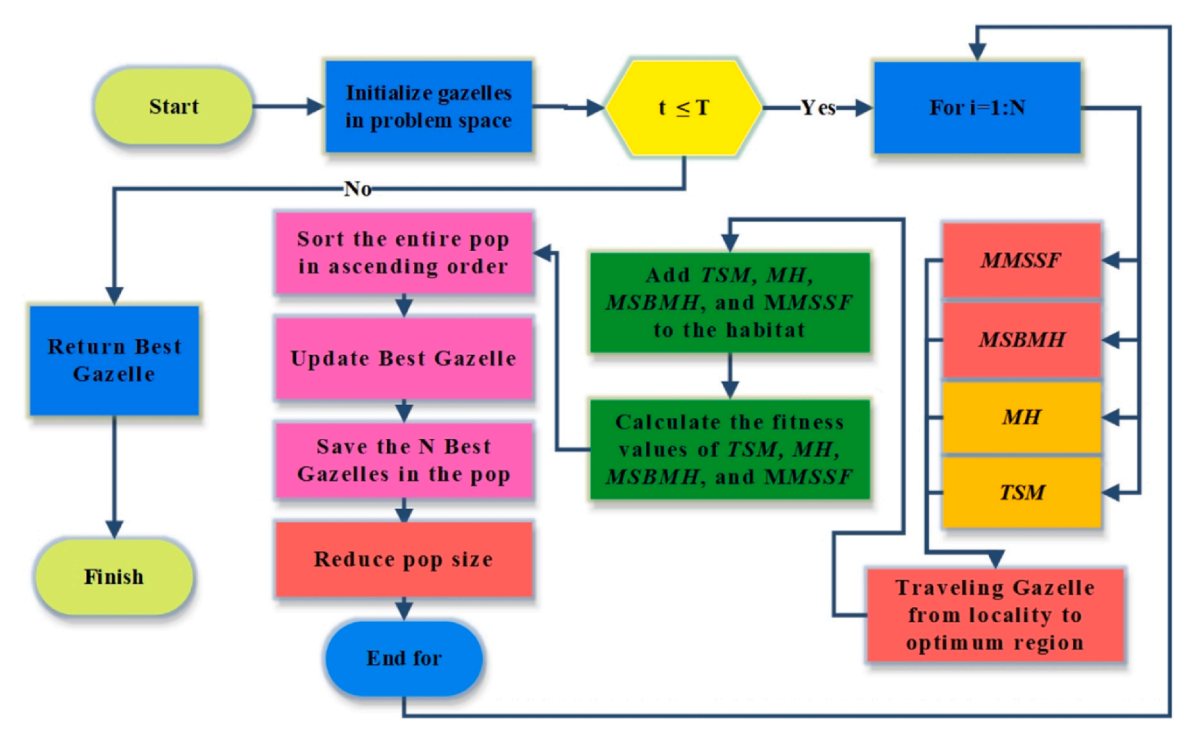


Fig. 2. Flowchart of the proposed IMGO.

(MLP) are radial basis function (RBF), feed-forward neural network (FFNN), cascade forward neural network (CFNN), general regression neural network (GRNN), and hybrid network [20,66]. Consequently, determining numbers of layers and nodes are crucial for designing a complicated nonlinear function. However, underfitting and overfitting challenges arise as a result of the growing number of nodes and improper selection of learning rate value [67]. Therefore, the architecture of the MFFNN has five distinct levels, including the input layer, three hidden layers, and the output layer. To effectively improve the data processing and training, the input data are normalized, the constant values in each row are omitted, the tansigmoidal activation function is chosen to handle regression difficulties [68], and the linear activation function is addressed for the output layer [69]. Consequently, the IMGO is employed to determine the most desirable numbers of neurons in the hidden layers  $(N_1, N_2, \text{ and } N_3)$  and optimum value of learning rate (LR). The data contains number of ambient temperature and solar radiation, whereas the final output is the PV system's output current. Finally, the polynomial regression integrated with  $IMGO_{MFFNN}$  to predict the output current.

#### 3.3.2. Polynomial regression (PR) model

The PR model is considered one of the most promising tool to predict the output variable based on independent input variables. PR model is a statistical algorithm which permits the numeric inputs to be numeric output [70]. In this paper, the PR model is integrated in the last stage to verify the accuracy between the actual and predicted current of the PV model by using Toolbox implemented in MATLAB software. The PR model offers a higher accuracy, especially when it is solved by using linear least square method, which is given by the following [64]:

$$y = \sum_{i=1}^{n+1} p_i x^{n+1-i} \tag{23}$$

where y is the response variable, x is the input variable (regressor), and n is the polynomial's degree and the order represents the number of coefficients to be fit. In this research, the 1st degree is computed to provide a high level accuracy of the predict output current using a linear least squares (LLS) approach, as given below:

$$f(x) = p_1 x + p_2 (24)$$

The main benefit of the polynomial models is that it has ability to fit the data that is not complicated. Hence, the nonlinearity of the input has been solved by  $IMGO_{MFFNN}$  model, while the poly fit model is employed for a precise fit for given data range.

#### 3.4. Model assessment criteria

This paper uses four statistical criteria to verify the performance of the proposed model: root mean square error (RMSE), mean bias error (MBE), coefficient of determination (R<sup>2</sup>), and absolute error (AE) [71,72]. RMSE defines the deviation scale between the predicted and target values and it is calculated by the following:

RMSE = 
$$\sqrt{\frac{1}{n} \sum_{i=1}^{n} (I_P - I_i)^2}$$
 (25)

MBE defines as the mean forecasted error is obtained to verify the average deviation the predicted and target values, which is given as follows:

$$MBE = \frac{1}{n} \sum_{i=1}^{n} I_{P} - I_{i}$$
 (26)

 $\rm R^2$  is defined as square of correlation between the predicted and target values, which is equal indicates highly correlated data and zero for non-correlated data, as represented by the following:

$$R^{2} = 1 - \frac{\sum_{i=1}^{n} (I_{P} - I_{i})^{2}}{\sum_{i=1}^{n} (I_{P} - \hat{I}_{i})^{2}}$$
(27)

where  $\hat{I}_i$  is the experimental current mean  $(\hat{I}_i = \frac{1}{n} \sum_{i=1}^n I_i)$ .

AE is presented for assessing the absolute deviation between the actual and predicted values and it is expressed as follows:

$$AE = |I_P - I_i| \tag{28}$$

The RMSE and MBE refer to the difference between the expected and actual data. Higher RMSE and MBE values indicate a greater variance in the expected and measured data, and vice versa. As a result, the

**Table 2**Technical specification of the PV model

Module type	STF-120P6
Rated power $(P_m)$	120 W
Short-circuit current $(I_{sc})$	7.63 A
Open-circuit voltage $(V_{oc})$	21.5 V
Current at MPP $(I_m)$	6.89 A
Voltage at MPP $(V_m)$	17.4 V
Temperature coefficient of $I_{sc}$ ( $\alpha$ )	6.93 mA%/°C
Temperature coefficient of $V_{oc}$ ( $\beta$ )	$-0.068  \text{V}/^{\circ} C$
Temperature coefficient of $P_m$ ( $\gamma$ )	-0.39 %

PV = photovoltaic.

model's accuracy is at its best when the RMSE and MBE values are close to zero. The linear relationship between the measured and anticipated results is assessed using  $R^2$  statistic. The closer  $R^2$  to one, the more accurate the model is. Finally, the AE describes the difference between the actual and expected model's output, a lower value of AE indicates a better level of accuracy [73].

#### 4. Experiment results and discussion

This section presents a description of the proposed  $IMGO_{PMFFNN}$  model by employing IMGO to optimize the hyperparameters of the MFFNN, including number of neurons in the hidden layers and

learning rate. Afterward, the polynomial model based on linear least squares is obtained for predicting the PV module's output current. This research uses 25 modules silicon PV titled at 15° and output current of (3 kWp) installed at the faculty of Engineering Built and Environment, Universiti Kebangsaan Malaysia with longitude value of 101.7713° and latitude value of 2.9210° [74]. The technical data of the PV model is tabulated in Table 2 [75]. The performance of the utilized in this work is six months of hourly meteorological data of the system, including solar radiation and ambient temperature. The system composes of transmitter of solar radiation of silicon PV detector (WE300) model with accuracy of  $\pm$  1%, sensor of temperature for the PV model's surface WE710 with accuracy of  $\pm$  0.25°C, sensor of air temperature WE700 model with range of - 50°C to 50°C and accuracy of ± 0.1°C, and current transducer CTH-050 model with input and output ranges of  $0 - 50 \,\mathrm{A}$  (DC) and  $4 - 20 \,\mathrm{mA}$  [74]. The hourly meteorological data input and output current are given in Fig. 3.

In this study, the data information is classified into two sections: 70% for training and 30% for testing [76]. The proposed models are IMGO<sub>MFFNN</sub>, IMGO<sub>MCFNN</sub>, IMGO<sub>RF</sub>, ALO<sub>RF</sub> [76], IMGO<sub>2ANN</sub>, ALO<sub>2ANN</sub> [27] applied to select the hyperparameters for the ANN and RF techniques. The population size is 30 and the maximum iteration is 100. The upper and lower hyperparameters for ANN method for the  $N_1$ ,  $N_2$ ,  $N_3$ , and LR are [1,25], [1,25], [1,25], and [0,1], respectively. Whereas the upper and lowers hyperparameters for RF method for the Numbers of trees ( $N_T$ ), leaves ( $N_L$ ), predictor ( $N_P$ ), and sample ( $N_S$ ) are [100,700], [10,100], [1,10], and [1,10], respectively. The authors of [76] optimized only numbers of trees and leaves. While, the

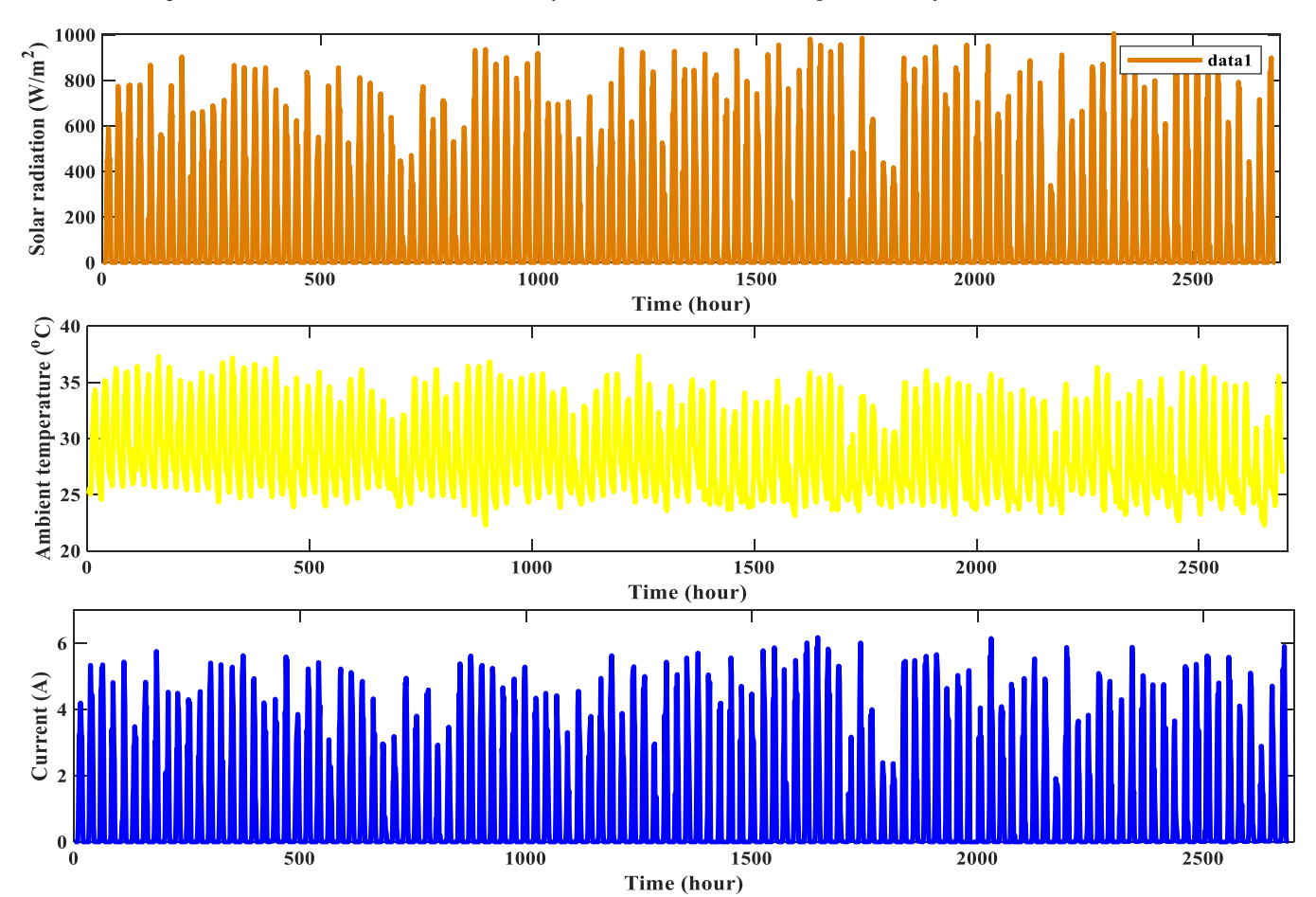


Fig. 3. The information dataset profile of utilized PV system. PV = photovoltaic.

**Table 3**Optimal hyperparameters using five models

Metho	d Hyperparameters	$\mathrm{IMGO}_{\mathrm{MFFNN}}$	$\mathrm{IMGO}_{\mathrm{MCFNN}}$	$\mathrm{IMGO}_{\mathrm{RF}}$	$ALO_{RF}$
ANN	LR	0.5661	0.0194	-	-
	$N_1$	2	11	-	-
	$N_2$	11	11	-	-
	$N_3$	7	1	-	-
RF	$N_{\mathrm{T}}$	-	-	571	681
	$N_L$	-	-	20	19
	$N_P$	-	-	10	
	N <sub>S</sub>	-	-	8	

ALO = ant lion optimizer; ANN = artificial neural network; MFFNN = multiple feed-forward neural network; RF = random forest; MCFNN = Multiple Layer Cascade Forward Neural Network.

authors of  $ALO_{2ANN}$  optimizes the weights and bias for only one hidden layer, which is set to be 12. Therefore, the optimal hyperparameters estimated by the mentioned models are presented in Table 3, while the optimized structure of the  $IMGO_{MFFNN}$  is shown in Fig. 4. For the DML models, the, LSTM [39], GRU [77], ELM [35], and LSSVM [78] are proposed for validation the performance of the proposed model, while their control parameter setting are given in Table 4.

The actual output current and the proposed models are demonstrated for the testing data in Fig. 5. As illustrated in zoomed figures, the proposed IMGO  $_{\rm MFFNN}$  model has closest prediction for the actual current compared with other models. It is worth to note that the predicted of the actual current is not straightforward task, this is because of the highly nonlinearity of the meteorological data, which are changeable during the day. However, the IMGO  $_{\rm MFFNN}$  model offers better accuracy, making it more suitable for predicting the PV model's output current. The ALO  $_{\rm 2ANN}$  exhibited poorest prediction of the PV output current, especially at maximum peak-energy during the day.

Table 4
Tuned control parameters of the DML models

Control parameter	ELM	GRU	LSSVM	CNN
Number of layers Number of iterations Number of nodes Activation function LR	500 5000 - RBF	1 5000 200 - 1e-8	- 5000 - RBF 1e-5	3 5000 20 ReLU 1e-8

CNN = convolutional neural network; ELM = extreme learning machine; GRU = gated recurrent unit; LSSVM = least square support vector machine; RBF = radial basis function.

The best RMSE, MSE, MBE, and R<sup>2</sup> are achieved by the IMGO<sub>MEENIN</sub> model, according to the Table 5, with statistical values of 0.0280, 7.8958E-4, -3.8184E-4, and 0.9951, respectively. For Central Processing Unit (Process time) (CPU) execution time, LSTM model yields the best time value with value of  $4.2\,s$ . The IMGO<sub>MCFNN</sub> and ELM models are ranked second, followed by IMGO<sub>2ANN</sub>, LSSVM, ALO<sub>2ANN</sub>, IMGO<sub>RF</sub>, ALORE, LSTM, and IMGO2ANN models, and GRU, where their statistical values are given in Table 5. The worst performance was registered by the CNN model. This is because of that CNN are hardly to handle longterm meteorological data. Moreover, it can be clearly seen that IM-GO<sub>2ANN</sub> model offers a better performance compared with ALO<sub>2ANN</sub> model, owning to affective employed exploration and exploitation tendencies in selecting proper set of the weight and bias, but the prediction of the PV output current using IMGO<sub>MFFNN</sub> model provides a higher accuracy and stability. Therefore, it can be concluded that developing the structure of the ANN model along with optimizing its hyperparameters can considerably provide a better prediction to the PV module's output current.

Similarly, the  $\mathrm{IMGO}_{\mathrm{RF}}$  provided more accuracy with slightly difference in terms of RMSE, MSE, MBE, and R² parameters as compared with  $\mathrm{ALO}_{\mathrm{RF}}$  models. This is because the IMGO model obtains powerful

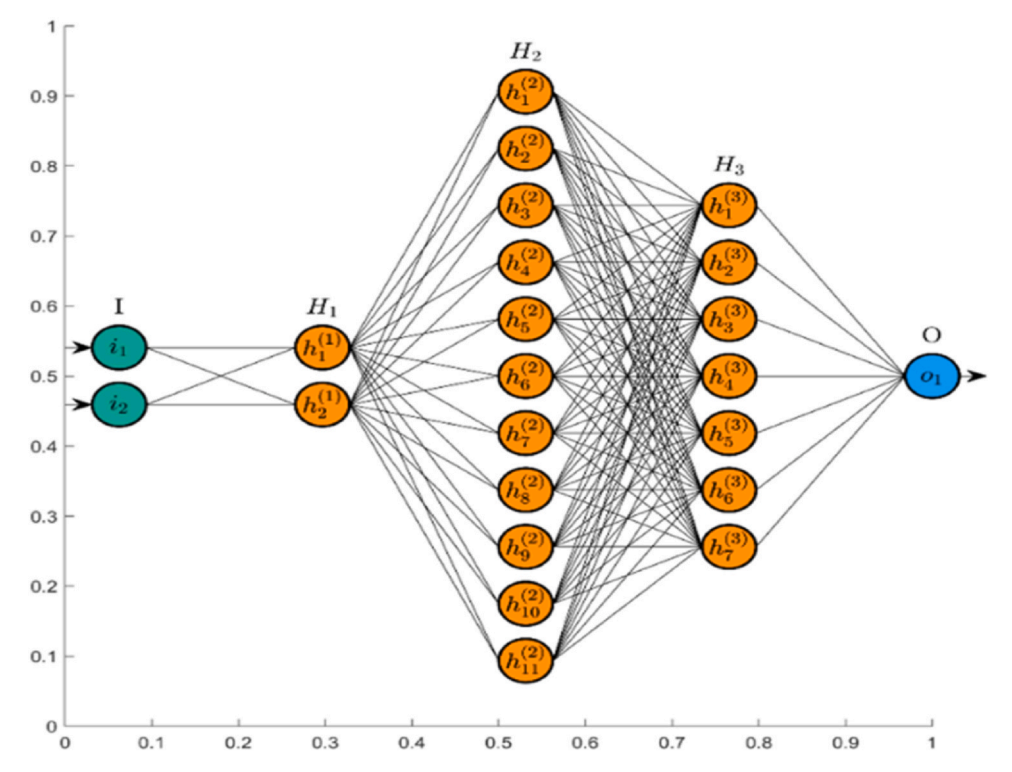


Fig. 4. Optimized architecture of the MFFNN using IMGO. MFFNN = multiple feed-forward neural network.

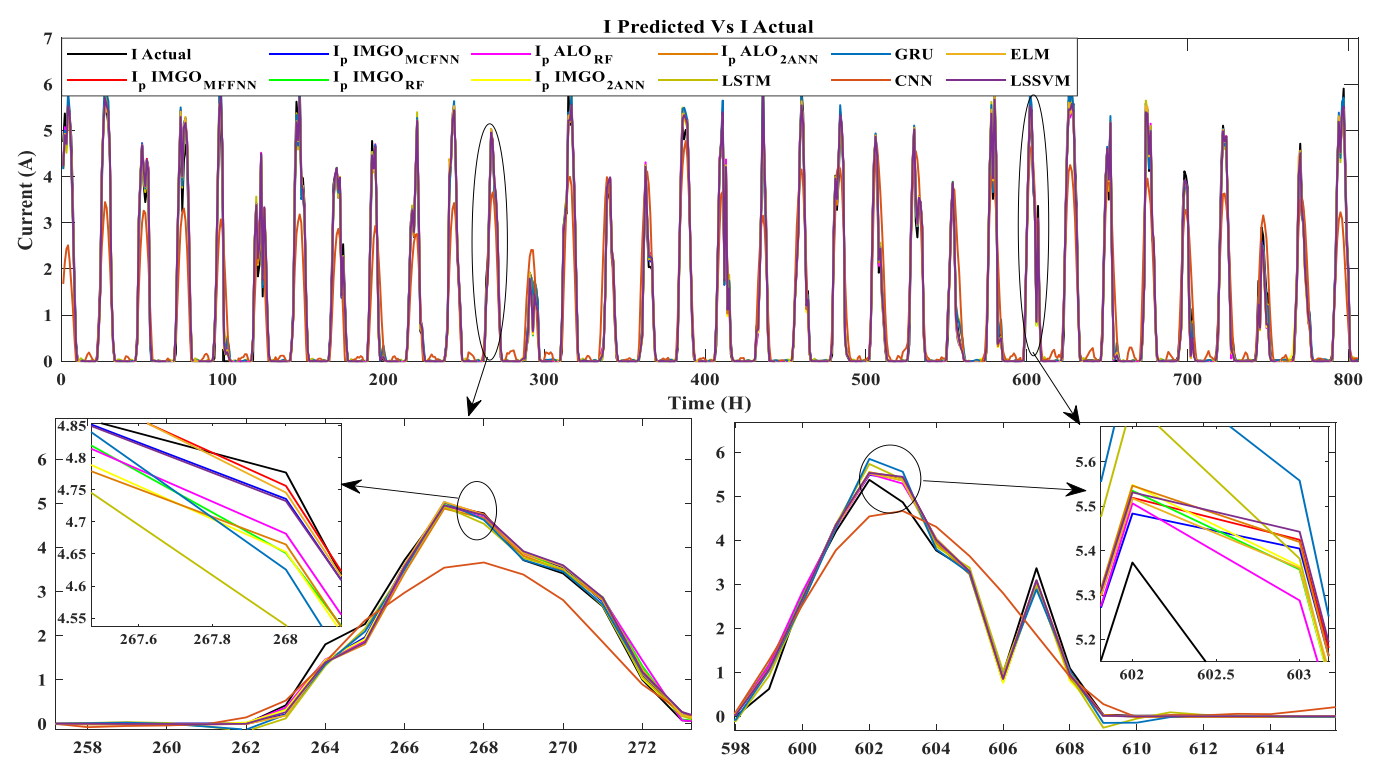


Fig. 5. Results of the forecasted PV system's output current using various models. PV = photovoltaic.

**Table 5**A comparison of statistical values using different models

Model	RMSE	MSE	MBE	$\mathbb{R}^2$	Time s
IMGO <sub>MFFNN</sub>	0.0280	7.8958E-4	-3.8184E-4	0.9951	24719.82
$IMGO_{MCFNN}$	0.0283	8.0603E-4	-9.9312E-4	0.9949	90944.92
$IMGO_{RF}$	0.0287	8.2595E-4	-0.00112	0.9948	488718.74
$ALO_{RF}$	0.0301	9.1109e-4	-0.00101	0.9942	135046.2
$IMGO_{2ANN}$	0.0289	8.3935e-4	0.00082	0.9946	259.2
$ALO_{2ANN}$	0.0292	8.5811e-4	0.00189	0.9945	120.3
LSTM	0.0321	0.001037	-8.166e-4	0.9935	4.2
GRU	0.0331	0.001099	-9.184E-4	0.9931	20099.3
LSSVM	0.0290	0.000845	-0.00135	0.9947	3127.0
ELM	0.0283	0.000806	-0.00151	0.9950	4.6
CNN	0.7810	0.610015	0.16194	0.9025	15128.2

ALO = ant lion optimizer; ANN = artificial neural network; CNN = convolutional neural network; ELM = extreme learning machine; GRU = gated recurrent unit; LSSVM = least square support vector machine; LSTM = long short-term memory; MBE = mean bias error; MFFNN = multiple feed-forward neural network; RF = random forest; RMSE = root mean square error.

The best model is pesented with Bold face.

strategies to select the most optimum hyperparameters for training RF, and it also optimizes the numbers of predictor and sample during the optimization process, which reflects a higher accuracy than  ${\rm ALO_{RF}}$  model. To end this, employing simply machine learning for forecasting the output current of the PV system might cause a serious problem for the gird rather leading to an increase in faults and costs.

Fig. 6, illustrates the scatter plot of the proposed IMGO $_{\rm MFFNN}$  and other models. The findings confirm the superiority of the IMGO $_{\rm MFFNN}$  among other models, followed by ELM model. From Fig. 6, it can be clearly seen that the correlation between the measured and

predicted currents are acceptable. However, a higher level of accuracy and stability is essential for the real applications of the PV system. This is because of that any mistakes or unsatisfied prediction may result more expenditure and directly impact on the stability for system.

Another important statistical criterion is AE, and it is evident from Fig. 7 that the  $\rm IMGO_{MFFNN}$  model has lower individual AE values than others models, indicating its superior ability for predicting the PV system's output current even at a variety of environmental circumstances. The highly unpredictable of solar radiation and ambient temperature may conduct noticeably larger errors in the PV model's

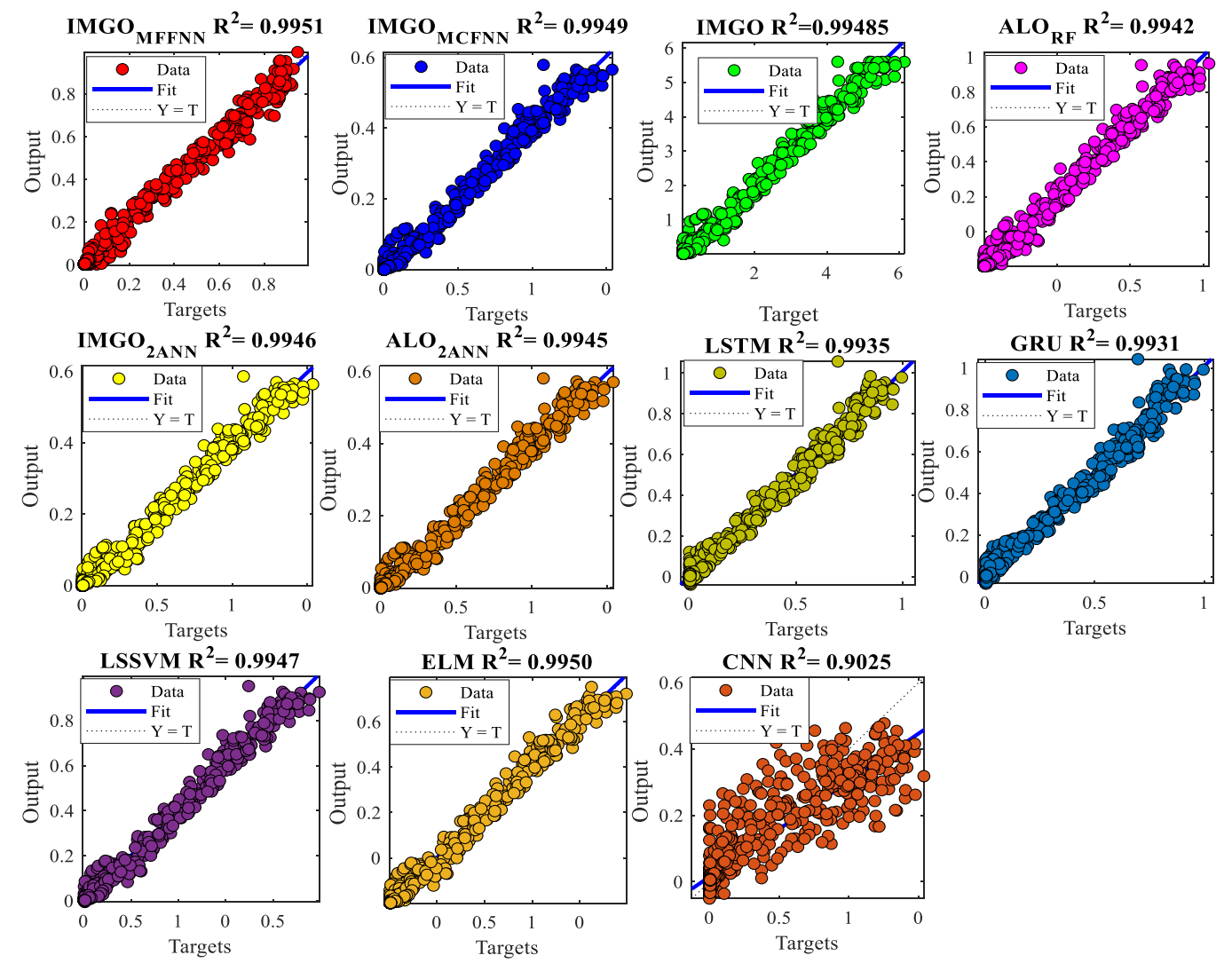


Fig. 6. Correlation between the actual and the predicted outputs in the testing data using various ML models. ML = machine learning.

forecasting of the output current, as seen in zoomed-figures. In comparison to other models, the  $\mathrm{IMGO}_{\mathrm{MFFNN}}$  model demonstrates a greater ability to minimize the error values. This is due the accurate implementation of learning algorithm of Bayesian Regularization backpropagation (BR) method, which reduces a combination of squared errors and weights synchronously. In addition to that the optimized number of hidden layers and learning rate considerably assist to boost the accuracy of the multiple layers neural network. Furthermore, its observed that the BR method performs better than Levenberg-Marquardt (LM) algorithm, but it takes longer processing time [68].

Finally, the development of the objective function (OF) using various models is depicted in Fig. 8. As a results, there are different formulations to minimize the OF values, where the  $IMGO_{MFFNN}$ ,  $IMGO_{MCFNN}$ ,  $IMGO_{RF}$ , and  $ALO_{RF}$  models optimize the hyperparameters of the ML methods, as shown on the parts (A) and (B). On contrast, the  $IMGO_{2ANN}$  and  $ALO_{2ANN}$  models enhance the weight and bias of the ANN, as presented on the part (C) of Fig. 8. It is apparent that the  $IMGO_{MFFNN}$  model has lowest RMSE value and needs the fewest iterations to obtain the optimal RMSE value. This is a result of

the significant advancements of the IMGO algorithm has undergone to predict the PV output current at a fast convergences rate. Moreover, compared to the  $IMGO_{RF}$  model, which has an OF value of 0.0288, the  $IMGO_{2ANN}$  provides a more precise set of weights and bias with a minimum value of 0.0113. Consequently, the implementation of the ANN yields a superiority compared with RF model with optimizing the hyperparameters of the both models. However, the IMGOFFNN model delivers a higher level of accuracy than other models for forecasting the output current of the PV model.

In the second stage, the estimated  $poly^1$  variables are given in the Table 6.

Fig. 9, demonstrates agreement between the actual and anticipated IMGO $_{PMFFNN}$  output current. It can be clearly observed that the IMG- $O_{PMFFNN}$  model presents a very high degree of accuracy and almost overlaps all the data points of the experimental data at various weather circumstances. The precision and dependability of the proposed IMG- $O_{PMFANN}$  model are illustrated in Fig. 10. The  $R^2$  value is extremely close to 1, and the residuals error has been significantly minimized, as seen in the top and bottom of the Fig. 10. Sum square error (SSE), RMSE, and  $R^2$  statistics for the IMGO $_{PMFFNN}$  model are tabulated in Table 7.

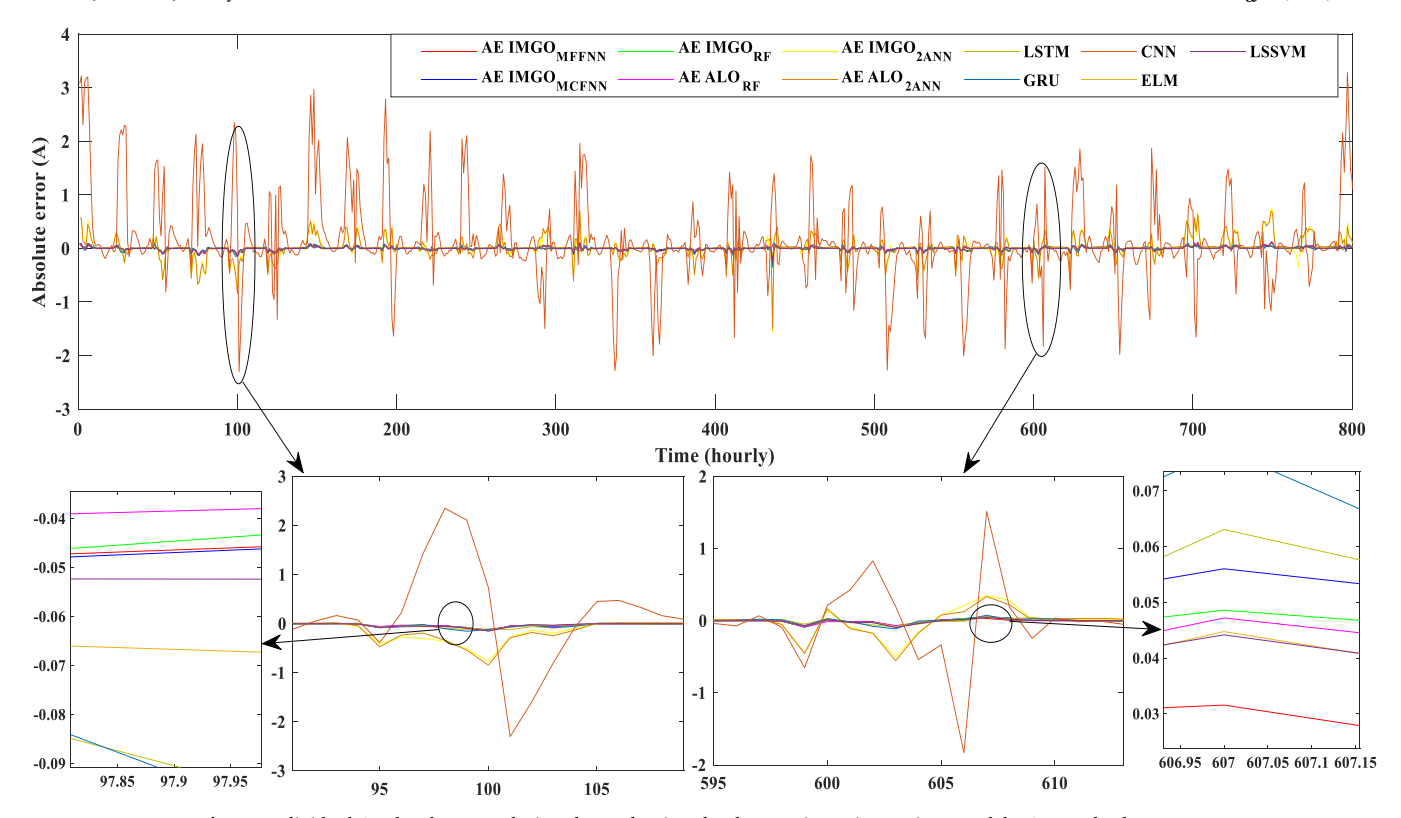


Fig. 7. Individual AE development during the evaluation the data testing using various models. AE = absolute error.

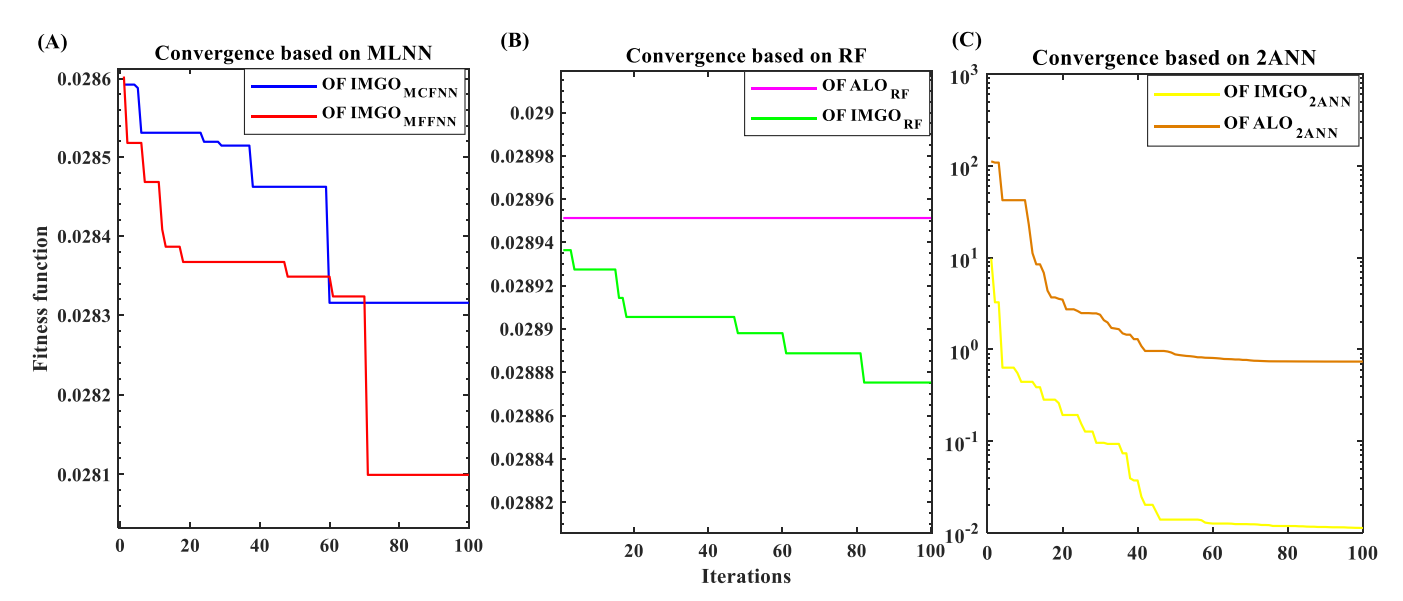


Fig. 8. Performance of the  $IMGO_{MFFNN}$ ,  $IMGOM_{MCFNN}$ ,  $IMGOM_{MCFNN}$ ,  $IMGOM_{ALO}$ , and  $ALO_{2ANN}$ , and  $ALO_{2ANN}$  models for minimizing the objective function. ALO = ant lion optimizer; ANN = artificial neural network; MFFNN = multiple feed-forward neural network; RF = random forest.

Table 6 Method and the predicted variables of the IMGO  $_{\rm PMFFNN}$  model

Fit type	Method	Coefficients	Value	Lower	Upper
Poly <sup>1</sup>	LLS	P1 P2	0.2790 0.1808	0.2789 0.1806	0.2792 0.1809

LLS = linear least squares.

The use of the IMGO as a metaheuristic algorithm to calculate the hyperparameters of the MFFNN model, which boosts its capacity to deliver an precise PV module's output. In addition, the inclusion of the  $\operatorname{Poly}^1$  regression model, in the second stage, utilizing LLS algorithm demonstrated that the proposed  $\operatorname{IMGO_{PMFFNN}}$  model provides a higher ability to predict the output current among other models.

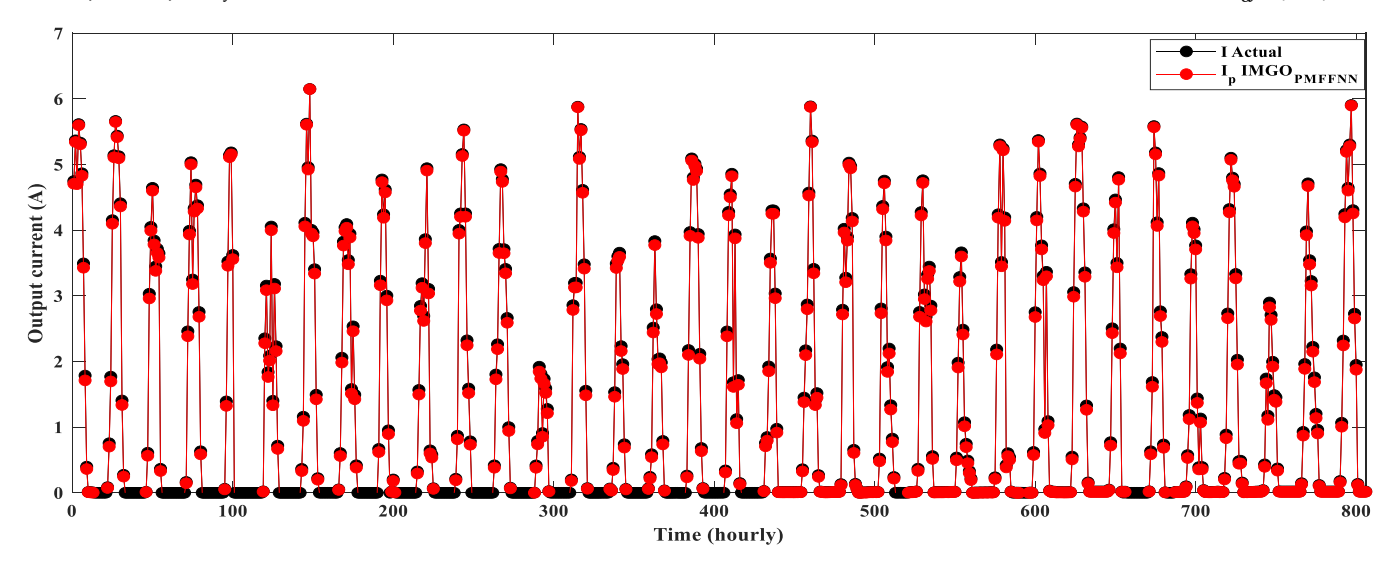


Fig. 9. A comparison between the predict current of Fit IMGOFFNN model and actual one.

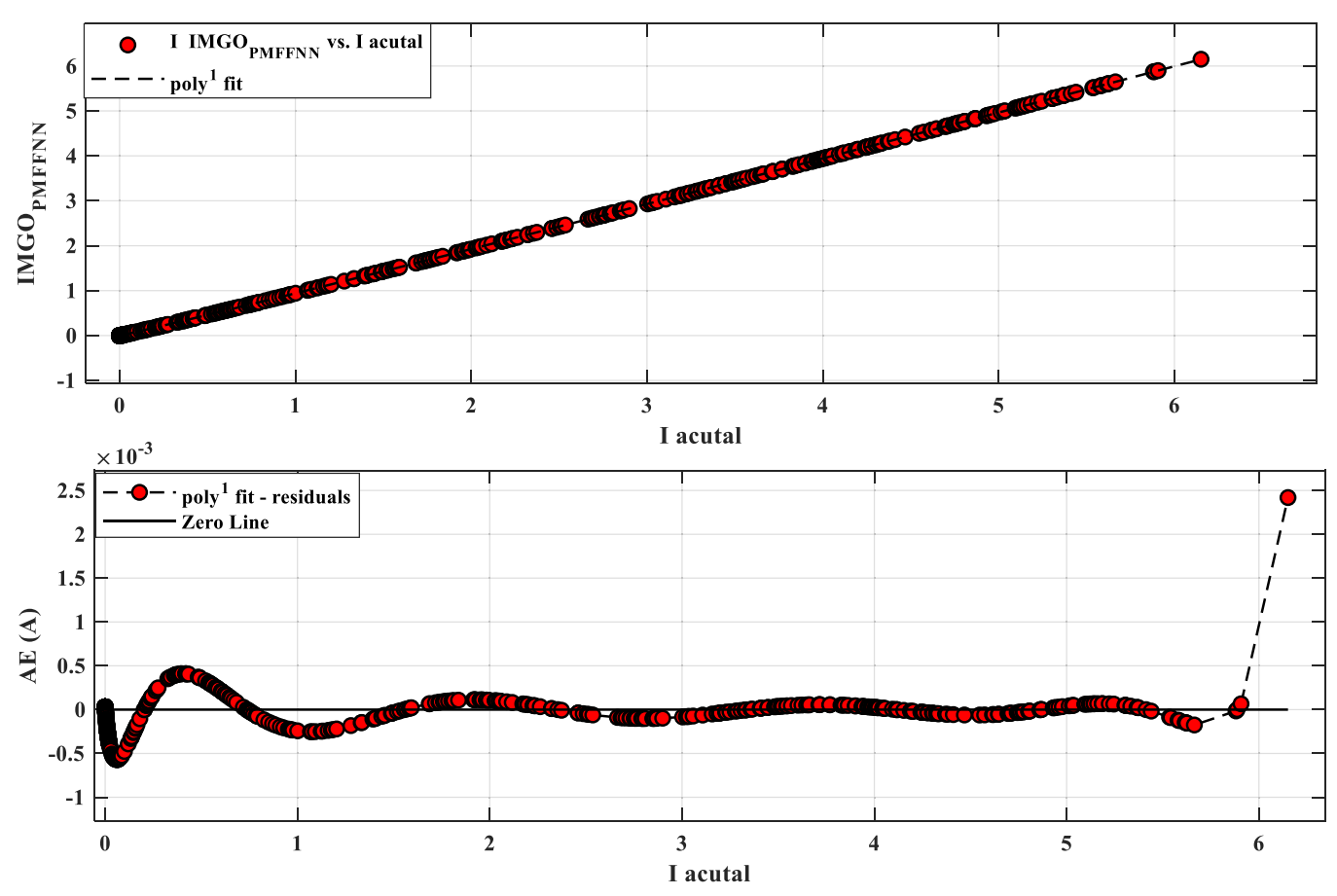


Fig. 10. Correlation between the predicted current and actual current.

**Table 7**Statistical values of the IMGO<sub>PMFFNN</sub> model

Model	Fit type	SSE	RMSE	R <sup>2</sup>
$IMGO_{PMFFNN}$	Poly <sup>1</sup>	0.0037	0.0021	0.9999

RMSE = root mean square error; SSE = sum square error; PMFFNN: Polynomial Model Forward Neural Network.

# 5. Conclusion and future direction

This study obtained actual hourly experimental data from Malaysia to offer a unique IMGO  $_{\rm PMFFNN}$  model to predict the PV module's output current. This work improved the original MGO for solving various kinds of engineering and predicting output current of the PV system problems. The trade-off between the exploration and exploitation are archived by developing the two main strategies MMSS, MSBMH, and accelerated convergence

curve. The IMGO is verified through 23 benchmark function and compared with famous meta-heuristic algorithms like original MGO, Opposition African Vulture Optimization Algorithm, Improved Sparrow Search Algorithm, DE, and PSO. The outcomes demonstrated that the IMGO performed excellently on the unimodal, multimodal, and fixed dimensional multimodal test functions. In addition, the proposed IMGO is investigated to solve six engineering problems, where the results indicated the efficiency and affectively implemented developments in handling difficult and constrained problems. Finally, the proposed IMGO is integrated with MFFNN based on 1st degree polynomial to predict the output current of the PV system using actual experimental data collected at Universiti Kebangsaan Malaysia, Malaysia. The proposed hybrid  $IMGO_{PMFFNN}$  model is compared with ant lion optimizer based on random forest ( $ALO_{RF}$ ) model, two stages of ANN (ALO $_{\rm 2ANN}$ ) model, LSTM, GRU, ELM, LSSVM, and CNN utilizing several statistical metrics. The experimental findings demonstrated that the proposed IMGO<sub>PMFFNN</sub> model can precisely predict the output current of the PV module and verified utilizing SSE, RMSE, and R<sup>2</sup> statistical criteria with values of 0.0037, 0.0021, and 0.999, respectively. It can be confirmed that the IMGO<sub>PMFENN</sub> model is more suitable for real-world applications of the PV system and can precisely simulate the actual behavior of the PV module

For future direction, the proposed IMGO can be hybridized with multiobjective optimization concept for solving conflicting objective functions. Furthermore, the output PV module's prediction can be further improved by utilizing hybrid DML model with PR model by improving its hyperparameters using advanced meta-heuristic method. This suggestion aims to not only improve the accuracy further, but also handle the longer processing time of the IMGO $_{\rm PMFFNN}$  model. In addition, the data preprocessing is essentially to reduce the noise and reducing the redundancy before employing Deep Machine Learning (DML) methods.

# CRediT authorship contribution statement

Hussein Mohammed Ridha: Conceptualization, Methodology, Resources, Writing – original draft, Writing – review & editing, Software, Formal analysis, Visualization, Investigation. Hashim Hizam: Writing – review & editing, Validation, Investigation, Formal analysis, Visualization, Supervision. Seyedali Mirjalili: Writing – review & editing, Methodology, Formal analysis, Visualization, Software, Investigation, Supervision. Mohammad Lutfi Othman: Formal analysis, Visualization, Investigation, Writing – review & editing. Mohammad Effendy Ya'acob: Formal analysis, Investigation, Visualization, Writing – review & editing. Noor Izzri Bin Abdul Wahab: Formal analysis, Investigation, Visualization, Writing – review & editing. Masoud Ahmadipour: Formal Analysis, Investigation, Visualization, Writing – review & editing.

#### **Declaration of Competing Interest**

The authors declare no conflict of interests for the publication of paper.

## Acknowledgments

The authors would like to thank Mustansiriyah University (www. uomustansiriyah.edu.iq) Baghdad-Iraq for their support of the present work.

#### Appendix A. Supporting material

Supplementary data associated with this article can be found in the online version at doi:10.1016/j.nxener.2025.100256.

#### References

[1] A. Agga, A. Abbou, M. Labbadi, Y. el Houm, Short-term self consumption PV plant power production forecasts based on hybrid CNN-LSTM, ConvLSTM models, Renew. Energy 177 (2021) 101–112, https://doi.org/10.1016/j.renene.2021.05. 095.

- [2] X.J. Dong, J.N. Shen, Z.F. Ma, Y.J. He, Simultaneous operating temperature and output power prediction method for photovoltaic modules, Energy 260 (2022) 1–12. https://doi.org/10.1016/j.energy.2022.124909.
- [3] M. Massaoudi, I. Chihi, H. Abu-Rub, S.S. Refaat, F.S. Oueslati, Convergence of photovoltaic power forecasting and deep learning: state-of-art review, IEEE Access 9 (2021) 136593–136615, https://doi.org/10.1109/ACCESS.2021.3117004.
- [4] A. Mellit, S. Kalogirou, Artificial intelligence and internet of things to improve efficacy of diagnosis and remote sensing of solar photovoltaic systems: challenges, recommendations and future directions, Renew. Sustain. Energy Rev. 143 (2021) 1–23, https://doi.org/10.1016/j.rser.2021.110889.
- [5] H.M. Ridha, H. Hizam, S. Mirjalili, M.L. Othman, M.E. Ya'acob, M. Ahmadipour, Parameter extraction of single, double, and three diodes photovoltaic model based on guaranteed convergence arithmetic optimization algorithm and modified third order Newton Raphson methods, Renew. Sustain. Energy Rev. 162 (2022) 112436, https://doi.org/10.1016/j.rser.2022.112436.
- [6] B. Cortés, R. Tapia Sánchez, J.J. Flores, Characterization of a polycrystalline photovoltaic cell using artificial neural networks, Sol. Energy 196 (2020) 157–167, https://doi.org/10.1016/i.solener.2019.12.012.
- [7] U.K. Das, K.S. Tey, M. Seyedmahmoudian, S. Mekhilef, M.Y.I. Idris, W. van Deventer, et al., Forecasting of photovoltaic power generation and model optimization: a review, Renew. Sustain. Energy Rev. 81 (2018) 912–928, https://doi.org/ 10.1016/j.rser.2017.08.017.
- [8] T. Shireen, C. Shao, H. Wang, J. Li, X. Zhang, M. Li, Iterative multi-task learning for time-series modeling of solar panel PV outputs, Appl. Energy 212 (2018) 654–662, https://doi.org/10.1016/j.apenergy.2017.12.058.
- [9] J. Fan, L. Wu, F. Zhang, H. Cai, W. Zeng, X. Wang, et al., Empirical and machine learning models for predicting daily global solar radiation from sunshine duration: a review and case study in China, Renew. Sustain. Energy Rev. 100 (2019) 186–212, https://doi.org/10.1016/j.rev.2018.10.018
- https://doi.org/10.1016/j.rser.2018.10.018.
   [10] X.J. Dong, J.N. Shen, G.X. He, Z.F. Ma, Y.J. He, A general radial basis function neural network assisted hybrid modeling method for photovoltaic cell operating temperature prediction, Energy 234 (2021) 1–10, https://doi.org/10.1016/j.energy.2021.121212.
- [11] L. Olatomiwa, S. Mekhilef, S. Shamshirband, D. Petković, Adaptive neuro-fuzzy approach for solar radiation prediction in Nigeria, Renew. Sustain. Energy Rev. 51 (2015) 1784–1791, https://doi.org/10.1016/j.rser.2015.05.068.
- [12] A.T. Eseye, J. Zhang, D. Zheng, Short-term photovoltaic solar power forecasting using a hybrid Wavelet-PSO-SVM model based on SCADA and meteorological information, Renew. Energy 118 (2018) 357–367, https://doi.org/10.1016/j.renene. 2017.11.011.
- [13] H. Zhen, D. Niu, K. Wang, Y. Shi, Z. Ji, X. Xu, Photovoltaic power forecasting based on GA improved Bi-LSTM in microgrid without meteorological information, Energy 231 (2021) 1–15, https://doi.org/10.1016/j.energy.2021.120908.
- [14] D. Markovics, M.J. Mayer, Comparison of machine learning methods for photovoltaic power forecasting based on numerical weather prediction, Renew. Sustain. Energy Rev. 161 (2022) 1–17, https://doi.org/10.1016/j.rser.2022.112364.
- [15] Q. Li, X. Zhang, T. Ma, C. Jiao, H. Wang, W. Hu, A multi-step ahead photovoltaic power prediction model based on similar day, enhanced colliding bodies optimization, variational mode decomposition, and deep extreme learning machine, Energy 224 (2021) 1–20, https://doi.org/10.1016/j.energy.2021.120094.
- [16] M. Ma, B. He, R. Shen, Y. Wang, N. Wang, An adaptive interval power forecasting method for photovoltaic plant and its optimization, Sustain. Energy Technol. Assess. 52 (2022) 1–10, https://doi.org/10.1016/j.seta.2022.102360.
- [17] H. Liu, Q. Gao, P. Ma, Photovoltaic generation power prediction research based on high quality context ontology and gated recurrent neural network, Sustain. Energy Technol. Assess. 45 (2021) 1–12, https://doi.org/10.1016/j.seta.2021.101191.
- [18] X. Ren, F. Zhang, H. Zhu, Y. Liu, Quad-kernel deep convolutional neural network for intra-hour photovoltaic power forecasting, Appl. Energy 323 (2022) 1–16, https:// doi.org/10.1016/j.apenergy.2022.119682.
- [19] L.L. Li, S.Y. Wen, M.L. Tseng, C.S. Wang, Renewable energy prediction: a novel short-term prediction model of photovoltaic output power, J. Clean. Prod. 228 (2019) 359–375, https://doi.org/10.1016/j.jclepro.2019.04.331.
- [20] M. Talaat, M.A. Farahat, N. Mansour, A.Y. Hatata, Load forecasting based on grasshopper optimization and a multilayer feed-forward neural network using regressive approach, Energy 196 (2020) 1–12, https://doi.org/10.1016/j.energy. 2020.117087.
- [21] L. Liu, Y. Zhao, D. Chang, J. Xie, Z. Ma, Q. Sun, et al., Prediction of short-term PV power output and uncertainty analysis, Appl. Energy 228 (2018) 700–711, https://doi.org/10.1016/j.apenergy.2018.06.112.
- [22] B. Gu, H. Shen, X. Lei, H. Hu, X. Liu, Forecasting and uncertainty analysis of dayahead photovoltaic power using a novel forecasting method, Appl. Energy 299 (2021) 1–14, https://doi.org/10.1016/j.apenergy.2021.117291.
- [23] I.A. Ibrahim, M.J. Hossain, B.C. Duck, An optimized offline random forests-based model for ultra-short-term prediction of PV characteristics, IEEE Trans. Ind. Inf. 16 (2020) 202–214, https://doi.org/10.1109/TII.2019.2916566.
- [24] X. Chen, K. Ding, J. Zhang, W. Han, Y. Liu, Z. Yang, et al., Online prediction of ultrashort-term photovoltaic power using chaotic characteristic analysis, improved PSO and KELM, Energy 248 (2022) 1–18, https://doi.org/10.1016/j.energy.2022.123574.
- [25] M.A. Hassan, N. Bailek, K. Bouchouicha, S.C. Nwokolo, Ultra-short-term exogenous forecasting of photovoltaic power production using genetically optimized nonlinear auto-regressive recurrent neural networks, Renew. Energy 171 (2021) 191–209, https://doi.org/10.1016/j.renene.2021.02.103.
- [26] A.K. Yadav, S.S. Chandel, Identification of relevant input variables for prediction of 1-minute time-step photovoltaic module power using Artificial Neural Network and Multiple Linear Regression Models, Renew. Sustain. Energy Rev. 77 (2017) 955–969, https://doi.org/10.1016/j.rser.2016.12.029.

- [27] S. Netsanet, D. Zheng, W. Zhang, G. Teshager, Short-term PV power forecasting using variational mode decomposition integrated with Ant colony optimization and neural network, Energy Rep. 8 (2022) 2022–2035, https://doi.org/10.1016/j.egyr. 2022.01.120.
- [28] F. Han, J. Jiang, Q.H. Ling, B.Y. Su, A survey on metaheuristic optimization for random single-hidden layer feedforward neural network, Neurocomputing 335 (2019) 261–273, https://doi.org/10.1016/j.neucom.2018.07.080.
- [29] L. Zhang, P.N. Suganthan, A survey of randomized algorithms for training neural networks, Inf. Sci. (NY) 364–365 (2016) 146–155, https://doi.org/10.1016/j.ins. 2016.01.039.
- [30] V.K. Ojha, A. Abraham, V. Snášel, Metaheuristic design of feedforward neural networks: a review of two decades of research, Eng. Appl. Artif. Intell. 60 (2017) 97–116, https://doi.org/10.1016/j.engappai.2017.01.013.
- [31] M. Jobayer, M.A.H. Shaikat, M. Naimur Rashid, M.R. Hasan, A systematic review on predicting PV system parameters using machine learning, Heliyon 9 (2023) e16815, https://doi.org/10.1016/j.heliyon.2023.e16815.
- [32] S. Sobri, S. Koohi-Kamali, N.A. Rahim, Solar photovoltaic generation forecasting methods: a review, Energy Convers. Manag. 156 (2018) 459–497, https://doi.org/ 10.1016/j.enconman.2017.11.019.
- [33] A. Mellit, S. Sağlam, S.A. Kalogirou, Artificial neural network-based model for estimating the produced power ofaphotovoltaic module, Renew. Energy 60 (2013) 71–78. https://doi.org/10.1016/j.renene.2013.04.011.
- [34] M. Trigo-González, F.J. Batlles, J. Alonso-Montesinos, P. Ferrada, J. del Sagrado, M. Martínez-Durbán, et al., Hourly PV production estimation by means of an exportable multiple linear regression model, Renew. Energy 135 (2019) 303–312, https://doi.org/10.1016/j.jrenep.2018.12.014
- [35] Z. Chen, H. Yu, L. Luo, L. Wu, Q. Zheng, Z. Wu, et al., Rapid and accurate modeling of PV modules based on extreme learning machine and large datasets of I-V curves, Appl. Energy 292 (2021) 1–19, https://doi.org/10.1016/j.apenergy.2021.116929.
   [36] S. Al-Dahidi, B. Hammad, M. Alrbai, M. Al-Abed, A novel dynamic/adaptive K-
- [36] S. Al-Dahidi, B. Hammad, M. Alrbai, M. Al-Abed, A novel dynamic/adaptive K-nearest neighbor model for the prediction of solar photovoltaic systems' performance, Results Eng. 22 (2024) 1–12, https://doi.org/10.1016/j.rineng.2024. 102141.
- [37] C.J. Huang, P.H. Kuo, Multiple-input deep convolutional neural network model for short-term photovoltaic power forecasting, IEEE Access 7 (2019) 74822–74834, https://doi.org/10.1109/ACCESS.2019.2921238.
- [38] S. Al-Dahidi, O. Ayadi, J. Adeeb, M. Alrbai, B.R. Qawasmeh, Extreme learning machines for solar photovoltaic power predictions, Energies (Basel) 11 (2018) 1–18, https://doi.org/10.3390/en11102725.
- [39] X. Qing, Y. Niu, Hourly day-ahead solar irradiance prediction using weather forecasts by LSTM, Energy 148 (2018) 461–468, https://doi.org/10.1016/j.energy. 2018.01.177.
- [40] D. Kothona, I.P. Panapakidis, G.C. Christoforidis, Day-ahead photovoltaic power prediction based on a hybrid gradient descent and metaheuristic optimizer, Sustain. Energy Technol. Assess. 57 (2023) 1–12, https://doi.org/10.1016/j.seta.2023.
- [41] Y. Yuan, Q. Yang, J. Ren, K. Li, Z. Wang, Y. Li, et al., Short-term wind power prediction based on IBOA-AdaBoost-RVM, J. King Saud. Univ. Sci. 36 (2024) 1–9, https://doi.org/10.1016/j.jksus.2024.103550.
- [42] N. Chopra, M. Mohsin Ansari, Golden jackal optimization: a novel nature-inspired optimizer for engineering applications, Expert Syst. Appl. 198 (2022) 1–15, https://doi.org/10.1016/j.eswa.2022.116924
- [43] L. Abualigah, D. Yousri, M. Abd Elaziz, A.A. Ewees, M.A.A. Al-qaness, A.H. Gandomi, Aquila optimizer: a novel meta-heuristic optimization algorithm, Comput. Ind. Eng. 157 (2021) 1–17, https://doi.org/10.1016/j.cie.2021.107250
- [44] D. Yousri, A. Fathy, H. Rezk, T. Sudhakar, M.R. Berber, A reliable approach for modeling the photovoltaic system under partial shading conditions using three diode model and hybrid marine predators-slime mould algorithm, Energy Convers. Manag. 243 (2021) 114269, https://doi.org/10.1016/j.enconman.2021.114269.
- [45] M.H. Hassan, S. Kamel, F. Jurado, U. Desideri, Global optimization of economic load dispatch in large scale power systems using an enhanced social network search algorithm, Int. J. Electr. Power Energy Syst. 156 (2024) 1–30, https://doi.org/10. 1016/j.ijepes.2023.109719.
- [46] E.H. Houssein, A.G. Gad, Y.M. Wazery, P.N. Suganthan, Task scheduling in cloud computing based on meta-heuristics: review, taxonomy, open challenges, and future trends, Swarm Evol. Comput. 62 (2021) 1–41, https://doi.org/10.1016/j. swevo.2021.100841.
- [47] G. Li, H. Hu, Risk design optimization using many-objective evolutionary algorithm with application to performance-based wind engineering of tall buildings, Struct. Saf. 48 (2014) 1–14, https://doi.org/10.1016/j.strusafe.2014.01.002.
- [48] B.A. Fadheel, N.I.A. Wahab, P. Manoharan, A.J. Mahdi, M.A.B.M. Radzi, A.B.C. Soh, et al., A hybrid sparrow search optimized fractional virtual inertia control for frequency regulation of multi-microgrid system, IEEE Access 12 (2024) 45879–45903, https://doi.org/10.1109/ACCESS.2024.3376468.
- [49] E. Çelik, A powerful variant of symbiotic organisms search algorithm for global optimization, Eng. Appl. Artif. Intell. 87 (2020) 1–14, https://doi.org/10.1016/j. engappai.2019.103294.
- [50] D.H. Wolpert, W.G. Macready, No free lunch theorems for optimization, IEEE Trans. Evolut. Comput. 1 (1997) 67–82, https://doi.org/10.1109/4235.585893.
- [51] Y. Yuan, Q. Yang, J. Ren, X. Mu, Z. Wang, Q. Shen, et al., Attack-defense strategy assisted osprey optimization algorithm for PEMFC parameters identification, Renew. Energy 225 (2024) 1–12, https://doi.org/10.1016/j.renene.2024.120211.
- [52] C. Ying, W. Wang, J. Yu, Q. Li, D. Yu, J. Liu, Deep learning for renewable energy forecasting: a taxonomy, and systematic literature review, J. Clean. Prod. 384 (2023) 1–49, https://doi.org/10.1016/j.jclepro.2022.135414.

- [53] A. Keddouda, R. Ihaddadene, A. Boukhari, A. Atia, M. Arıcı, N. Lebbihiat, et al., Solar photovoltaic power prediction using artificial neural network and multiple regression considering ambient and operating conditions, Energy Convers. Manag. 288 (2023) 1–15, https://doi.org/10.1016/j.enconman.2023.117186.
- [54] P. Malik, R. Chandel, S.S. Chandel, A power prediction model and its validation for a roof top photovoltaic power plant considering module degradation, Sol. Energy 224 (2021) 184–194, https://doi.org/10.1016/j.solener.2021.06.015.
- [55] B. Abdollahzadeh, F.S. Gharehchopogh, N. Khodadadi, S. Mirjalili, Mountain Gazelle optimizer: a new nature-inspired metaheuristic algorithm for global optimization problems, Adv. Eng. Softw. 174 (2022) 1–34, https://doi.org/10.1016/j. advenosoft 2022 103282
- [56] S. Das, S.S. Mullick, P.N. Suganthan, Recent advances in differential evolution-an updated survey, Swarm Evol. Comput. 27 (2016) 1–30, https://doi.org/10.1016/j. swevo.2016.01.004.
- [57] S.Y. Park, J.J. Lee, Stochastic opposition-based learning using a beta distribution in differential evolution, IEEE Trans. Cyber 46 (2016) 2184–2194, https://doi.org/10. 1109/TCYB.2015.2469722.
- [58] G. He, X. li Lu, Quasi opposite-based learning and double evolutionary QPSO with its application in optimization problems, Eng. Appl. Artif. Intell. 126 (2023) 1–21, https://doi.org/10.1016/j.engappai.2023.106861.
- [59] A. Faramarzi, M. Heidarinejad, S. Mirjalili, A.H. Gandomi, Marine predators algorithm: a nature-inspired metaheuristic, Expert Syst. Appl. (2020) 113377, https://doi.org/10.1016/j.eswa.2020.113377.
- [60] N.E. Humphries, N. Queiroz, J.R.M. Dyer, N.G. Pade, M.K. Musyl, K.M. Schaefer, et al., Environmental context explains Levy and Brownian movement patterns of marine predators, Nature 465 (2010) 1066–1069, https://doi.org/10.1038/ nature09116.
- [61] R.N. Mantegna, Fast, accurate algorithm for numerical simulation of Lévy stable stochastic processes, Phys. Rev. E 49 (1994) 4677–4683, https://doi.org/10.1103/ PhysRevE.49.4677.
- [62] X.-S. Yang, Engineering Optimisation: An Introduction with Metaheuristic Applications, John Wiley and Sons, 2010, https://onlinelibrary.wiley.com/doi/ book/10.1002/9780470640425.
- [63] L. Abualigah, A. Diabat, S. Mirjalili, M. Abd Elaziz, A.H. Gandomi, The arithmetic optimization algorithm, Comput. Methods Appl. Mech. Eng. 376 (2021) 113609, https://doi.org/10.1016/j.cma.2020.113609.
- [64] T.M. Alabi, E.I. Aghimien, F.D. Agbajor, Z. Yang, L. Lu, A.R. Adeoye, et al., A review on the integrated optimization techniques and machine learning approaches for modeling, prediction, and decision making on integrated energy systems, Renew. Energy 194 (2022) 822–849, https://doi.org/10.1016/j.renene.2022.05.123.
- [65] E. Çelik, Y. Uzun, E. Kurt, N. Öztürk, N. Topaloğlu, A neural network design for the estimation of nonlinear behavior of a magnetically-excited piezoelectric harvester, J. Electron. Mater. 47 (2018) 4412–4420, https://doi.org/10.1007/s11664-018-6078-2
- [66] R. Ahmed, V. Sreeram, Y. Mishra, M.D. Arif, A review and evaluation of the state-of-the-art in PV solar power forecasting: techniques and optimization, Renew. Sustain. Energy Rev. 124 (2020) 1–26, https://doi.org/10.1016/j.rser.2020.109792.
- [67] D. Tien Bui, V.H. Nhu, N.D. Hoang, Prediction of soil compression coefficient for urban housing project using novel integration machine learning approach of swarm intelligence and multi-layer perceptron neural network, Adv. Eng. Inform. 38 (2018) 593–604, https://doi.org/10.1016/j.aei.2018.09.005.
- [68] R. Khalid, N. Javaid, A survey on hyperparameters optimization algorithms of forecasting models in smart grid, Sustain. Cities Soc. 61 (2020) 1–25, https://doi. org/10.1016/j.eec.2020.102275
- [69] K.G. Sheela, S.N. Deepa, Review on methods to fix number of hidden neurons in neural networks, Math. Probl. Eng. 2013 (2013) 1–12, https://doi.org/10.1155/ 2013/425740.
- [70] A. Mellit, S. Sağlam, S.A. Kalogirou, Artificial neural network-based model for estimating the produced power ofaphotovoltaic module, Renew. Energy 60 (2013) 71–78, https://doi.org/10.1016/j.renene.2013.04.011.
- [71] J. Zhang, Z. Tan, Y. Wei, An adaptive hybrid model for day-ahead photovoltaic output power prediction, J. Clean. Prod. 244 (2020) 1–10, https://doi.org/10. 1016/j.jclepro.2019.118858.
- [72] T. Ahmad, H. Chen, A review on machine learning forecasting growth trends and their real-time applications in different energy systems, Sustain. Cities Soc. 54 (2020) 1–27, https://doi.org/10.1016/j.scs.2019.102010.
- [73] S. Al-Dahidi, O. Ayadi, M. Alrbai, J. Adeeb, Ensemble approach of optimized artificial neural networks for solar photovoltaic power prediction, IEEE Access 7 (2019) 81741–81758. https://doi.org/10.1109/ACCESS.2019.2923905.
- [74] I.A. Ibrahim, T. Khatib, A. Mohamed, W. Elmenreich, Modeling of the output current of a photovoltaic grid-connected system using random forests technique, Energy Explor. Exploit. 36 (2018) 132–148, https://doi.org/10.1177/0144598717723648.
- [75] T. Khatib, W. Elmenreich, Modeling of Photovoltaic Systems Using Matlab: Simplified green codes, John Wiley & Sons, 2016, https://onlinelibrary.wiley.com/doi/book/10.1002/9781119118138.
- [76] I.A. Ibrahim, M.J. Hossain, B.C. Duck, An optimized offline random forests-based model for ultra-short-term prediction of PV characteristics, IEEE Trans. Ind. Inf. 16 (2020) 202–214, https://doi.org/10.1109/TII.2019.2916566.
- [77] P. Li, K. Zhou, X. Lu, S. Yang, A hybrid deep learning model for short-term PV power forecasting, Appl. Energy 259 (2020) 1–11, https://doi.org/10.1016/j.apenergy. 2019 114216
- [78] M. Gao, J. Li, F. Hong, D. Long, Day-ahead power forecasting in a large-scale photovoltaic plant based on weather classification using LSTM, Energy 187 (2019) 1–12, https://doi.org/10.1016/j.energy.2019.07.168.